Earth-Science Reviews 112 (2012) 155–172

Contents lists available at SciVerse ScienceDirect

Earth-Science Reviews

journal homepage: www.elsevier.com/locate/earscirev

What controlled Mid–Late Miocene long-term aridification in Central Asia? — Global cooling or Tibetan Plateau uplift: A review

Yunfa Miao [a,c,*], Mark Herrmann [b], Fuli Wu [c], Xiaoli Yan [d,c], Shengli Yang [e,c]

[a] Key Laboratory of Desert and Desertification, Cold and Arid Regions Environmental and Engineering Institute, Chinese Academy of Sciences, Lanzhou 730000, China
[b] Senckenberg Research Institute and Natural History Museum, Senckenberganlage 25, D-60325 Frankfurt/Main, Germany
[c] Key Laboratory of Continental Collision and Plateau uplift, Institute of Tibetan Plateau Research, Chinese Academy of Sciences, Beijing 100085, China
[d] Key Laboratory of Western China's Environmental Systems, Ministry of Education & Research School of Arid Environment and Climate Change, Lanzhou University, Lanzhou, 730000, China
[e] College of Geographical Sciences, Nanjing Normal University, Nanjing, Jiangsu 210046, China

ARTICLE INFO

Article history:
Received 11 July 2011
Accepted 16 February 2012
Available online 24 February 2012

Keywords:
Miocene
Central Asia
Global cooling
Tibetan Plateau
Aridification
Long-trend

ABSTRACT

Debate continues over whether global cooling or uplift of the Tibetan Plateau provided the first-order driver for the aridification (moisture levels) of Central Asia throughout the Mid–Late Miocene, between about 17 and 5 Ma. This review attempts to throw new light on the relations between the aridification and these two key factors. This paper examines the evolution of Miocene climate (both moisture and temperature) within five separate regions of Eurasia to help understand the large scale controls of long-term moisture in Central Asia. The five regions include: (1) Europe, (2) high-latitude Asia, (3) the East Asian Monsoon region, (4) the South Asian Monsoon region, and (5) Central Asia itself, because moisture reaching Central Asia has to firstly cross at least one of the other four regions. Temperature proxy data compiled from these five regions correlate with ocean temperatures from the global deep-sea oxygen isotope records. Furthermore, compiled moisture proxy data from the four regions surrounding Central Asia co-vary and correlate with each other. This can be explained by positive feedbacks between drying and cooling, and supports the assumption that global cooling provides a dominant driving factor for the drying of Eurasia: global cooling reduces the amount of water vapor held in the atmosphere and thereby can cause terrestrial drying. However, in Central Asia the moisture evolution shows less similarity with its surroundings. The uplift of the Tibetan Plateau (including the Tianshan Mountains) could provide a possible explanation for this difference. The changing topography resulting from uplift events over time and space strongly influenced the moisture patterns in Central Asia during Miocene times. Future research on the spatial timing and amplitude of Tibetan Plateau uplift should be useful to understand the moisture processes in Central Asia during the Miocene.

© 2012 Elsevier B.V. All rights reserved.

Contents

1. Introduction . . . 156
2. Physical geography and precipitation patterns of Eurasia . . . 157
3. Data sources and methods . . . 159
   3.1. Study region and site selection . . . 159
   3.2. Temperature and moisture indices and statistical analysis . . . 159
4. Temperature and moisture records . . . 160
   4.1. Europe . . . 160
   4.2. High latitude Asia (and Alaska) . . . 161
   4.3. East Asian Monsoon region . . . 161
   4.4. South Asian Monsoon region . . . 162
   4.5. Central Asia . . . 163
5. Discussion . . . 164
   5.1. Common climatic trends of Eurasia . . . 164
   5.2. Influence of global cooling on Eurasian climate trends . . . 164

* Corresponding author at: Cold and Arid Regions Environmental and Engineering Institute, Chinese Academy of Sciences, Lanzhou 730000, China. Tel.: +86 9314967544; fax: +86 9314967659.
E-mail address: Miaoyunfa@lzb.ac.cn (Y. Miao).

0012-8252/$ – see front matter © 2012 Elsevier B.V. All rights reserved.
doi:10.1016/j.earscirev.2012.02.003

5.3. Influence of Tibetan Plateau uplift on Central Asian climate trends . . . 165
5.3.1. Northwestern Tibetan Plateau (Tianshan region) . . . 166
5.3.2. Northeastern Tibetan Plateau . . . 166
5.4. Influence of the Asian monsoon, Paratethys, and other factors on Central Asian climate trends . . . 168
6. Summary and conclusions . . . 169
Acknowledgments . . . 169
References . . . 169

1. Introduction

Widespread deserts and semi-deserts (e.g., the Gobi Desert) characterize the natural landscape of Central Asia, in contrast to high mountain areas (Fig. 1). The evolution of climate within these environments has influenced the vegetation history of Inner Asia since Miocene times. Even today, these dominant geographical features of Asia strongly affect millions of people. Understanding the origination, development and driving forces behind this landscape and climate hence provide essential understanding for the future of Central Asia. Consequently, many investigations focus on this region. Especially during the past two decades, scientists have summarized data from oil exploration and stratigraphic studies and realized the fundamental ecological and climatic pattern change at the Oligocene/Miocene boundary. This change is characterized by a climatic turnover from arid to humid conditions in eastern China and the restriction of arid conditions to northwestern China (e.g., Wang, 1984; Liu et al., 1998; Sun and Wang, 2005; Zhang and Guo, 2005; Guo et al., 2008). Studies of wind-blown silt sediments (loess and red clay) deposited in North and Central China have provided knowledge about the environmental changes of Central Asia since Early Miocene times (Liu, 1985; Ding et al., 1998; Sun et al., 1998; Guo et al., 2002; 2008; Qiang et al., 2011). Many of these studies have focused on the basic scientific question of what controlled the aridification of Central Asia since the Miocene? Based on studies of proxy data (e.g., Zhang, 1981; Li and Fang, 1999; An et al., 2001; Fang et al., 2007; Sun et al., 2009) and modeling (Manabe and Terpstra, 1974; Kutzbach et al., 1989; Ruddiman and Kutzbach, 1989; Manabe and Broccoli, 1990; Raymo and Ruddiman, 1992; Liu et al., 2003) one theory dominated: that the stepwise uplift of the Tibetan Plateau (mostly) following the India–Asia collision directly drove the stepwise aridification of Inner Asia during the late Cenozoic. The retreat of the shallow Paratethys Sea was also identified as an important feature for the precipitation decrease in Central Asia (Ramstein et al., 1997; Zhang et al., 2007). However, other researchers suggest that global cooling controlled the stepwise drying in interior Asia by reducing the amount of

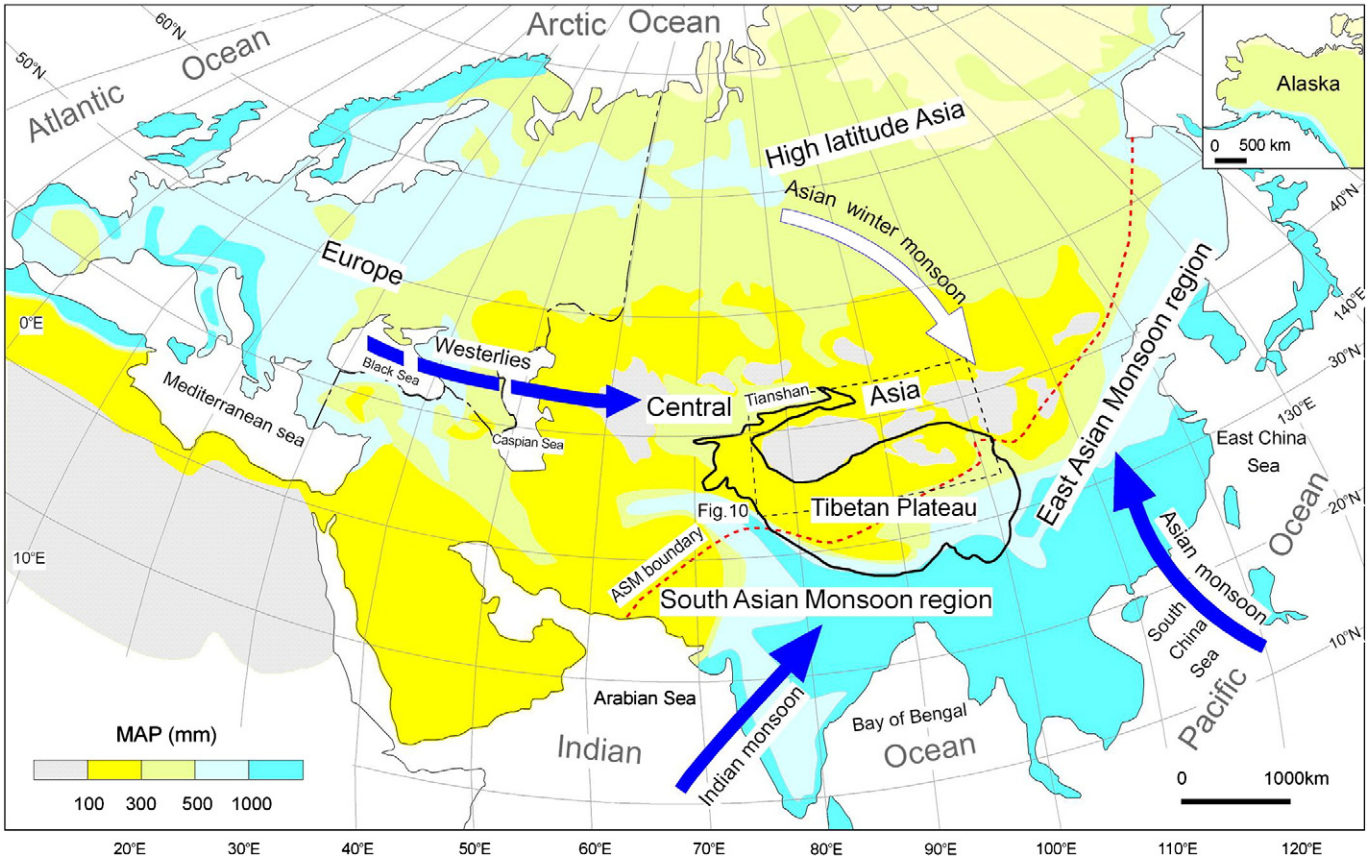

Fig. 1. Physical geography and distribution of precipitation throughout Eurasia. The four main precipitation resources that influence Central Asia follow: 1) Atlantic Ocean moisture brought by the Westerlies, 2) the Western Pacific, 3) Indian Ocean moisture brought by the East Asian Monsoon, and South Asian Monsoon, and 4) moisture from the Asian winter monsoon. The modern Asian summer monsoon (ASM) limit is shown by a red dashed line (after Gao, 1962). Dashed rectangle is illustrated by Fig. 10 in more detail.

water vapor held in the atmosphere, and that the growth of the Tibetan Plateau played only a subordinate role (Chen et al., 1990; Wang and Gao, 1990; Guo et al., 1998; 2004; Liu and Ding, 1998; Dupont-Nivet et al., 2007; Jiang and Ding, 2008; Passey et al., 2009; Lu et al., 2010; Wan et al., 2010; Miao et al., 2011a; Tang et al., 2011). Recently, new data have been published regarding the precipitation/the effective moisture (precipitation minus evaporation) development of Eurasia (e.g., Mosbrugger et al., 2005; Velichko et al., 2005; Utescher et al., 2007a,b; Clift et al., 2008; Jiménez-Moreno et al., 2008, 2010; Sun and Zhang, 2008; Jiménez-Moreno et al., 2010; Wan et al., 2010; Hui et al., 2011; Liu et al., 2011; Miao et al., 2011a; Qiang et al., 2011; Tang et al., 2011; Zhang and Sun, 2011). Reviewing and comparing these new research works with older data can help to identify the first order control causing the aridification of Central Asia throughout the Miocene. This review relies mainly on climatic records based on macro- and microscopic plant remains (as well as some other climatic proxies) from 38 sites in Eurasia and neighboring areas (see locations in Fig. 2 and sites information in Table 1). Our focus lies on using publications of data and ideas from locations within: (1) Europe, (2) high-latitude Asia, (3) the East Asian Monsoon region (4) the South Asian Monsoon region, and (5) Central Asia itself, to illustrate the relationships between continental temperatures, deep sea temperatures, and precipitation patterns, and investigate the relationships between global cooling and the evolution of moisture on a continental scale. If global cooling provided the main control for the stepwise drying of interior Asia by reducing the amount of water vapor held in the atmosphere, the climatic patterns of our five investigated regions should show similar trends of temperature and moisture development to the global climate itself. This paper attempts to document the patterns of global cooling and effective moisture evolution by bringing together plant fossil data (as well as other climatic proxies) to evaluate and understand the factors controlling the aridification of Central Asia on a long time scale during the Miocene.

2. Physical geography and precipitation patterns of Eurasia

Today, Eurasia stretches over 8000 km in width, including points north of the Arctic Circle and south of the equator, covering nearly half of the northern hemisphere. The eastern and western coasts of Eurasia experience very different climatic conditions, influenced by the prevailing atmospheric and oceanic circulation systems. Marine conditions generally control the climate of western Eurasia, which is influenced by the Gulf Stream. With distance from coast, the climate becomes more continental. The East Asian Monsoon mainly controls the climate of East Asia and reaches eastern China Mainland, Japan, North Korea, South Korea, and Taiwan. Warm and wet summer monsoon conditions prevail, along with cold and dry winter monsoon conditions. In south Asia however, the South Asian Monsoon affects India and the Indochina Peninsula, bringing large amounts of precipitation inland into East Asia. In Central Asia, a strong seasonality dominates the climate conditions, with varying temperatures and low precipitation. Large areas of open landscape, dominated by grasslands, make up the interior vegetation in the middle latitudes of Eurasia. The Tibetan Plateau, an immense upland measuring more than 3500 across by 1500 km wide in size, averages more than 5000 m in elevation, lies in the middle latitudes of Eastern Asia (Fig. 1). The Tibetan Plateau strongly influences circulation patterns of the Asian monsoon. The high mountains at the south of the Plateau cut off the winds and hence the moisture transport from the Indian Ocean, as well as the Pacific Ocean, resulting in arid regions in eastern Central Asia. Currently, the humid areas of Eurasia lie mainly in

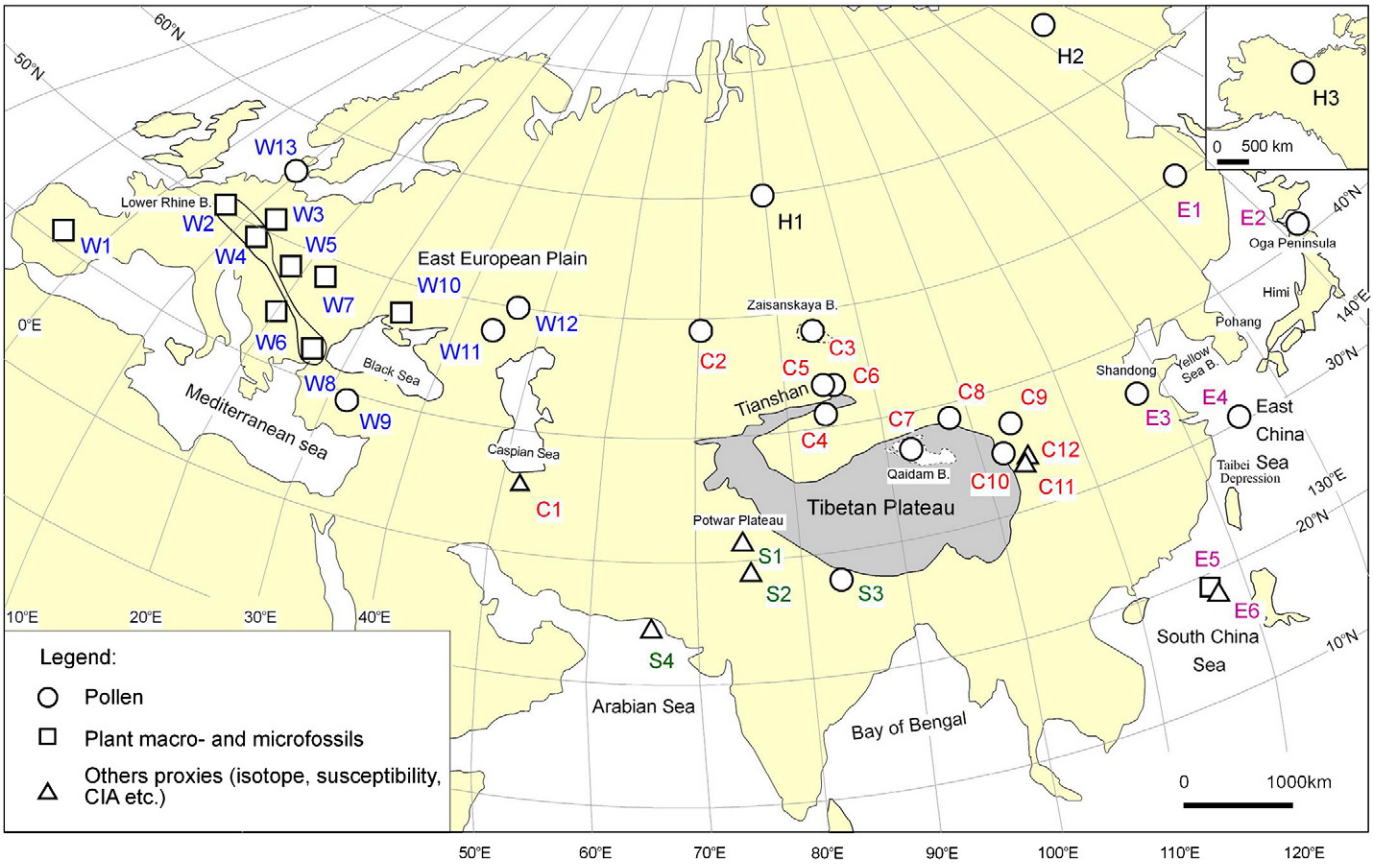

Fig. 2. Overview map showing the palaeoclimatic sites selected in this study from Europe (W1–W13), High latitude Asia (H1–H3), East Asian Monsoon region (E1–E6), South Asian Monsoon region (S1–S5), and Central Asia region (C1–C12) (see Table 1 for sites information and references).

Table 1
Detailed information about reviewed publications.

Site no.	Location	Lat. (°N)	Lon. (°E)	Sample	Time period	Age control	Climatic proxies used	Climatic information	Reference
W1	Calatayud–Teruel Basin	41	−1.5	Out.	18–5 Ma	Bio.	Meg.	MAT MAP	Barrón et al. (2010)
W2	Lower Rhine Basin	50.8 −51.1	6.4 −6.8	Wells	Mio.	Bio.	Meg.	MAT MAP	Utescher et al. (2000) and Utescher et al. (2009)
W3	Weisselster and Lausitz Basin	52	12	Wells	Mio.	Bio.	Meg.	MAT MAP	Mosbrugger et al. (2005) and Utescher et al. (2009)
W4	Austria	47.6 −48.6	14.0 −16.1	Out.	E.-M. Mio.	Stra.	Pol. Meg.	MAT MAP	Jiménez-Moreno et al. (2008)
W5	Pannonian domain	46.5 −48.2	16.5 −21.1	Wells Out.	Mio.	Bio. Rad.	Meg.	MAT MAP	Erdei et al. (2007)
W6	Serbia	44.8 −43.9	20.2 −22.2	Out.	Mio.	Bio.	Meg.	MAT MAP	Utescher et al. (2007a)
W7	Ukraine Carpathians	48.0 −48.4	22.6 −23.7	Wells Out.	Mio.	Bio.	Mic.	MAT MAP	Syabryaj et al. (2007)
W8	Bulgaria region	41.4 −43.9	22.6 −28.2	Cores Out.	Mio.	Bio. Mag. Rad.	Meg. Mic.	MAT MAP	Ivanov et al. (2011)
W9	Turkey	36–41	27–45	Out.	Mio.	Bio.	Pol.	P/A ratio MAP	Akgün et al. (2007) and Akkiraz et al. (2011)
W10	Ukraine Plain	45.3 −46.8	30.5 −34.0	Wells	Mio.	Bio.	Meg. Mic.	MAT MAP	Syabryaj et al. (2007)
W11	SE Russian Plain	45 −52	39 −45	Out.	Mio.	Bio.	Pol.	QT QM	Velichko et al. (2005)
W12	SE East European Plain	46 −53	41 −50	Out.	Mio.	Bio.	Pol.	MAT	Velichko et al. (2005)
W13	Sdr. Vium, Denmark	55.8	8.4	core	19–8	p	Pol.	MAT MAP	Larsson et al., 2011
H1	West Siberia, Russia	60	80	Out. Cores	Mio.	Bio. Mag.	Pol.	QT	Arkhipov et al. (2005)
H2	NE Asia, Russia	66	142	Cores	Mio.	Bio. Mag.	Pol.	MAT	Fradkina et al. (2005)
H3	Alaska, USA	63.9 −69.2	135.3 −163.1	Out. Cores	18–0 Ma	Bio. Mag. Rad.	Pol.	MAT QT QM	White et al. (1997)
E1	South Far East	50	136	Out.	Mio.	Bio. Rad.	Pol.	QT	Korotky et al. (2005)
E2	Oga Peninsula, Japan	40	140	Out.	13–2 Ma	Bio.	Pol.	QT	Wang et al. (2001)
E3	Shandong, North China	36.5 −37.8	117.4 −118.9	Out. Cores	Mio.	Bio. Mag. Rad.	Pol.	QT QM	Wang (1996)
E4	East China Sea	28 −32.5	124 −126	Cores	Mio.	Pol.	Pol.	QT QM	Hu and Sarjeant (1992)
E5	ODP 1146, South China Sea	19.45	116.27	Core	24–0 Ma	Mag. Bio.	CIA	QM	Wan et al. (2007) and Wan et al. (2010)
E6	ODP 1148, South China Sea	18.83	116.55	Core	24–0 Ma	Mag. Bio.	$\delta^{18}O$ CIA	QT QM	Wang et al. (2003), Wei et al. (2006) and Clift (2006)
S1	Potwar Plateau	33	73	Out.	<18–0 Ma	Bio. Mag.	$\delta^{18}O$	QM	Quade et al. (1989, 1995)
S2	North India	30.3 −32.0	75.7 −77.2	Out.	~11–2 Ma	Bio. Mag.	$\delta^{18}O$	QM	Sanyal et al. (2004, 2005)
S3	Surai Khola, Central Nepal	28	83	Out.	11.5–<1 Ma	Bio. Mag.	Pol.	QT QM	Hoorn et al. (2000)
S4	Well Indus Marine A-1	24.2	67.6	Core	17–3 Ma	Bio. Mag.	CIA	QM	Clift et al. (2008)
C1	North Iran	52.2	35.5	Out.	E.-M. Mio.	Mag.	$\delta^{18}O$	QM	Ballato et al. (2010)
C2	North and west Kazakhstan	45 −50	58 −80	Out.	Mio.	Bio.	Pol.	MAT MAP	Akhmetyev et al. (2005)
C3	Zaisanskaya Basin	48	83.9	Out.	Mio.	Bio.	Pol.	MAT MAP	Akhmetyev et al. (2005)
C4	Kuchetawu, Tianshan Range	41.9	83.5	Out.	13.3–2.6 Ma	Mag.	Pol.	QT QM	Zhang and Sun (2011)
C5	Jingouhe, Tianshan	44.2	85.5	Out.	28–4.2 Ma	Mag.	Pol.	QT QM	Tang et al. (2011)
C6	Taxihe, Tianshan Range	44.1	86.3	Out.	26.5–2.6 Ma	Mag.	Pol.	QT QM	Sun and Zhang (2008)
C7	KC-1, Qaidam Basin	38.01	91.75	Core	18–5	Strat.	Pol.	QT QM	Miao et al. (2011a)
C8	Laojunmiao, Jiuquan Basin	39.5	97.5	Out.	13.0–2.2 Ma	Mag.	Pol.	QT QM	Ma et al. (2005)
C9	Sikouzi, Ningxia	36.3°	106.2	Out.	<~20 Ma	Mag. Bio.	Pol.	QM	Jiang et al. (2007) and Jiang and Ding (2008)
C10	Maogou, Linxia Basin	35.6	103.3	Out.	30.5–5.0 Ma	Mag. Bio.	Pol.	QT QM	Ma et al. (1998) and Fang et al. (2003)

Table 1 (*continued*)

Site no.	Location	Lat. (°N)	Lon. (°E)	Sample	Time period	Age control	Climatic proxies used	Climatic information	Reference
C11	Qin'an, Tianshui Basin	35.0	105.4	Out.	22–6.2 Ma	Mag. Bio.	MS	QM	Guo et al. (2002)
C12	ZL, Zhuanglang	35.2	106.0	Cores	25.6–4.8 Ma	Mag.	MS	QM	Qiang et al. (2011)

Out.-Outcrop; Mio.-Miocene; Bio.-Biostratigraphy; Mag.-Magnetostratigraphy; Strat.-Stratigraphical correlation. MS: Magnetic Susceptibility QT: Qualitative Temperature; QM: Qualitative Moisture; Rad.-Radiometric data; Meg.-Megafloras; Mic.-Microfloristic plant; Pol.-Pollen; CIA: Chemical Index of Alteration.

regions affected by the East Asian Monsoon and South Asian Monsoon, but also include Western Europe and the northern margin of Western Africa, all of which have mean annual precipitations of more than 1000 mm (Fig. 1). Semi-humid areas (mean annual precipitation between 500 mm and 1000 mm) lie along the north-eastern margin of Asia, and include most of Europe. Semi-arid areas (mean annual precipitation between 300 mm and 500 mm) stretch over western Asia and include most of northern Asia. The most arid regions (mean annual precipitation between 100 mm and 300 mm) fall mainly in middle Asia, between 30° and 50° N; and the center of this region is characterized by extremely arid conditions (mean annual precipitation <100 mm). Overall, the precipitation in Eurasia exhibits increasing aridity depending on the distance from the coast (Fig. 1). Westerly air masses driven by the Corriolis force provide the main sources of moisture for western Asia, nearly reaching the Tibetan Plateau. East and South Asia, however, derive moisture from the Pacific Ocean and the Indian Ocean, respectively.

3. Data sources and methods

3.1. Study region and site selection

The geographical region considered in this review covers the entire Eurasian continent, as well as the surrounding lands (Fig. 1). The five regions, which differ with respect to modern climate patterns, including: (1) Europe (and much of western Asia) mainly influenced by the Westerlies, (2) high-latitude Asia (plus Alaska) mainly affected by the Siberian High, (3) the East Asian Monsoon region, dominated by the East Asian Monsoon, (4) the South Asian Monsoon region, dominated by the South Asian Monsoon, and (5) Central Asia, influenced from all sides.

Abundant climatic proxies in these regions (e.g., megafloras, pollen, mammals, oxygen isotopes, major and trace elements, chemical weathering index, magnetic susceptibility, etc.) span the various time periods with available data of variable quality. This study selected primarily plant fossil sites characterized by continuous records covering the whole or at least the main portion of the Miocene, with no great depositional hiatus. A total of 38 sedimentary sites met these criteria and have been used within this study (Table 1). Organized by their geographical positions (the five regions above) to make the discussion more convenient, the analyses come from the referenced publications. This review presents and discusses the temperature and moisture developments that are representative for climate changes within these regions. The authors provide climatic proxy data or they have been digitized from diagrams within their publications.

3.2. Temperature and moisture indices and statistical analysis

Long-term climatic trends have been reconstructed, although reviewed publications have used a number of different climatic proxies and reconstruction methods (Table 1) — for example, the Coexistence Approach (Mosbrugger and Utescher, 1997). The Coexistence Approach allows quantitative reconstruction of the mean annual temperature, the temperature of the coldest month and the mean annual precipitation (e.g., Utescher et al., 2000; Mosbrugger et al., 2005; Erdei et al., 2007; Syabryaj et al., 2007; Utescher et al., 2007a; Jiménez-Moreno et al., 2008; Utescher et al., 2009; Barrón et al., 2010; Akkiraz et al., 2011; Ivanov et al., 2011; and Popova et al., 2011). Pollen data of floras can be used for more qualitative temperature reconstructions: for example, the percentages of thermophilic pollen taxa, the percentages of tropical pollen taxa, the percentages of xerophytic taxa, the ratios of trees preferring warm versus cold conditions, or the ratios of arctotertiary/palaeotropical elements (e.g., Ma et al., 1998; Hoorn et al., 2000; Ma et al., 2005; Akgün et al., 2007; Akkiraz et al., 2011; Miao et al., 2011a). Other methods used include principal component analysis (PCA, an ordination technique) of the pollen data for qualitative reconstruction of temperature and moisture (Jiang and Ding, 2008; Sun and Zhang, 2008; Tang et al., 2011; Zhang and Sun, 2011), the humidity index (percentages of the arid plants divided by the non-arid plants) (Jiang and Ding, 2008), grassland percentages (Hoorn et al., 2000; Miao et al., 2011a), or the canopy density (White et al., 1997).

Further methods provide supplementary data for the understanding of the climate change include the use of: (1) the Chemical Index of Alteration (CIA), (2) $\delta^{18}O$ values from soil carbonate, and (3) magnetic susceptibility of loess sediments as effective moisture proxies. The CIA serves as a standard proxy for the intensity of chemical weathering in sediments, based on the concentrations of water-immobile Al (Aluminum) relative to Na (Sodium), K (Potassium) and Ca (Calcium). For example, sediments from the Bay of Bengal and from the South China Sea have been successfully linked to the intensity of the Asian monsoon (e.g., Clift, 2006; Wei et al., 2006; Wan et al., 2007; Clift et al., 2008; Wan et al., 2010). The records of $\delta^{18}O$ from soil carbonate (Quade et al., 1989; 1995; Sanyal et al., 2004; 2005; Ballato et al., 2010) are also useful for precipitation reconstruction. Measuring magnetic susceptibility on loess sediments of Northwest China has been widely used to classify the intensity of the Asian summer precipitation (e.g., Kukla et al., 1988; An et al., 1991, 2000; Guo et al., 2002; Vandenberghe et al., 2004; Qiang et al., 2011). For temperature conditions additional, we also used one $\delta^{18}O$ record from benthic foraminifera to represent temperature conditions (Wang et al., 2003). However, many temperature and moisture reconstructions result from proxy studies and provide only relative comparisons and are only usable in a semi-quantitative sense, referring to the individual sites. The exceptions include results of the Coexistence Approach (Mosbrugger and Utescher, 1997), mean annual temperatures, the temperatures of the coldest month, and mean annual precipitation.

The example shown in Fig. 3 illustrates how we derived our reconstructions of the long-term development of temperature and moisture. For comparison, we used the compiled oxygen isotope records of Zachos et al. (2008), which reflect the globally averaged temperature undergoing a gradually cooling trend (Fig. 3a, red arrow). Based on the proxies used in the reviewed articles, we show the results from a pollen record from the Qaidam Basin, Central Asia (Fig. 2, location C7) (Miao et al., 2011a), which reconstructs temperature and precipitation trends during the late Early to Late Miocene (Fig. 3b, c; red and blue arrows). We have used a heuristic approach to draw the linear regression lines. Here the percentages of the thermophilic taxa remain high between 18 and 14 Ma and decrease after

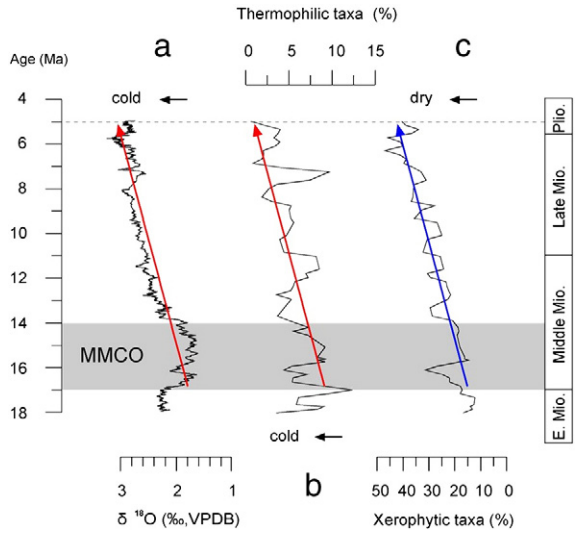

Fig. 3. (a) Compiled Miocene oceanic $\delta^{18}O$ records (after Zachos et al., 2008) and their average trend (red arrow). (b) Qualitative temperature record with average trend (red arrow) and (c) moisture record with average trend (blue arrow) of the KC-1 core from the Qaidam Basin, Central Asia (adapted from Miao et al., 2011a). The gray rectangle denotes the Middle Miocene Climatic Optimum (MMCO) at ~17–14 Ma (Flower and Kennett, 1994).

that period, a pattern which corresponds well with the global climatic cooling trend (Fig. 3b). During the same period, xerophytic taxa percentages gradually increase, suggesting aridification (Fig. 3c).

4. Temperature and moisture records

4.1. Europe

Abundant research activity in Europe on micro- and macro-plant records of various time periods provides a basis for examining its history of Miocene climate change in detail. By using the Coexistence Approach (Mosbrugger and Utescher, 1997), available data have been combined to reconstruct the European long term trends of climate change during Miocene. Fig. 4 (location W1) shows the mean annual temperature and mean annual precipitation results, based on vegetation data from the Iberian Peninsula (Barrón et al., 2010). A slight decrease in precipitation can be identified although the temperature remained stable. In the Lower Rhine Basin, northwest Germany (Fig. 2, location W2), records cover the interval between 26 and 2 Ma (Berggren et al., 1995); in which the mean annual temperatures show a comparatively warm interval in the Middle Miocene (~17–14 Ma), with cooling beginning at about 14 Ma. Precipitation rates show related trends (wet during the warm period and dry during the cold period, with strong fluctuations) to those of the reconstructed data of the mean annual temperature (Utescher et al., 2000; Mosbrugger et al., 2005) (Fig. 4W2). The development of Miocene (~23–9 Ma) temperatures in the Weisselster Basin and the Lausitz Basin of northeast Germany corresponds to the global oceanic oxygen isotope record (Zachos et al., 2001), and precipitation rates again show related trends to those of the mean annual temperature (Mosbrugger et al., 2005; Utescher et al., 2009) (Fig. 4, location W3). Jiménez-Moreno et al. (2008) reconstructed a warm, humid subtropical climate for Austria during the mid-Miocene (ca. 18–10 Ma) characterized by a cooling trend together with a slight increase of the mean annual precipitation (Fig. 4, location W4). Erdei et al. (2007) provides a survey regarding the Pannonian (area of Hungary and Yugoslavia) domain Miocene vegetation and its climate history based on selected fossil plant assemblages. They recognized a slight general cooling and drying trend (Fig. 4W5). Utescher et al. (2007a) show a cooling and drying trend during the entire investigated time period in Serbia, using the Coexistence Approach (Fig. 4W6). Samples from the Ukrainian Carpathians (Fig. 4W7) and the Ukraine Plain (Fig. 4W10) yield similar climatic trends, wherein the development of temperature and precipitation runs from high values to low values, expressing a general cooling and drying trend, although it seems that precipitation trends

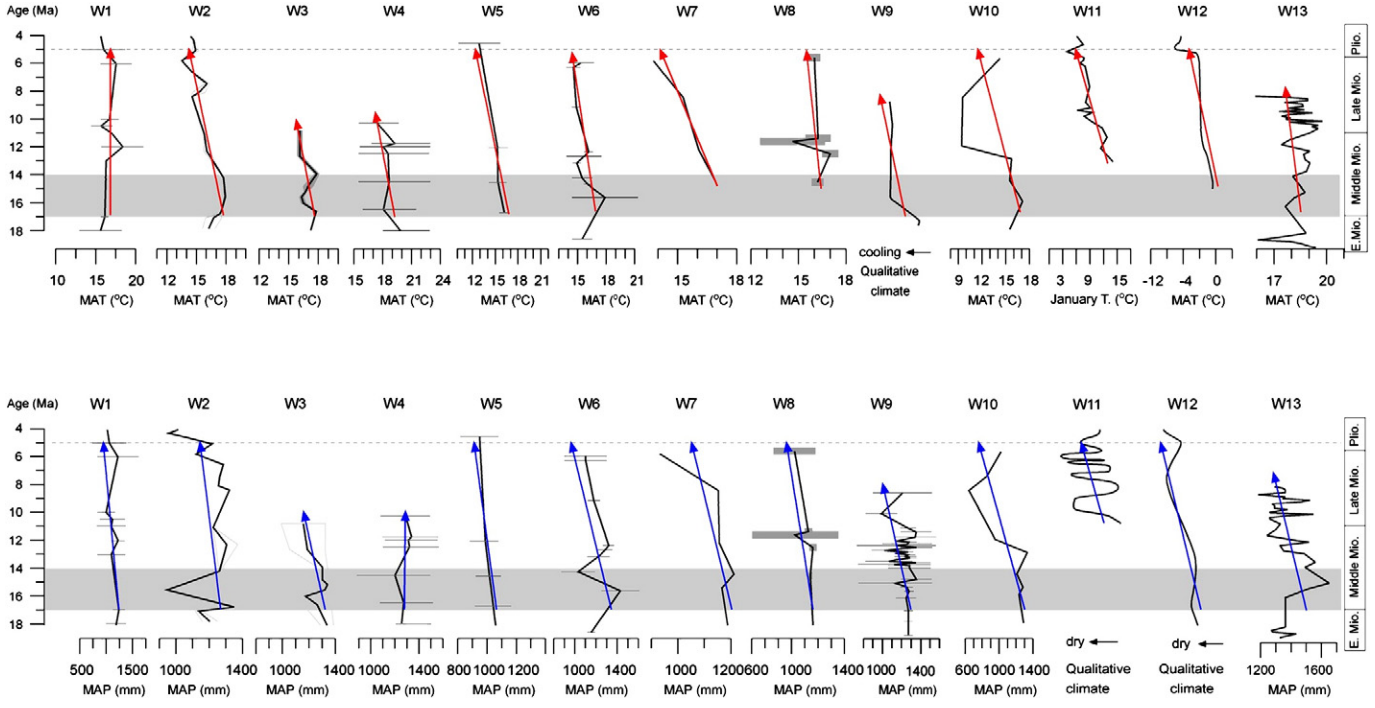

Fig. 4. Variations and long-term trends in European climate during Mid–Late Miocene: upper part, temperature; lower part, precipitation. Red arrows indicate temperature trends, blue arrows indicate aridity trends. The gray rectangle highlights the Middle Miocene Climatic Optimum. MAT: mean annual temperature, MAP: mean annual precipitation.

fluctuate more than the temperature ones (Syabryaj et al., 2007). Ivanov et al. (2011; based on the Coexistence Approach) found that mean annual temperature and mean annual precipitation in Bulgaria show trends roughly similar to the other locations (Fig. 3W8). Akgün et al. (2007) applied the Coexistence Approach on samples from Turkey spanning from ~25 to 9 Ma and found that both temperature and precipitation trends seem somewhat similar to the global change throughout the Mid–Late Miocene (Fig. 3W9), findings also supported by recently published palynological results of Akkiraz et al. (2011). Palynological samples from the Russian platform (Velichko et al., 2005; Fig. 4W11), spanning the time from 13–11 Ma to ~5 Ma, show continuously falling winter temperatures (January), together with strongly fluctuating aridification trends. Temperatures on the East European Plain (Fig. 4W12) decreased during the Middle to Late Miocene, while precipitation also fell continuously during the Miocene (Velichko et al., 2005). Recently, Larsson et al. (2011) determined mean annual temperatures and mean annual precipitation based on pollen data from Denmark, northern Europe, that show decreasing trends between ~19 and 8 Ma (Fig. 3W13). Totally, almost all sites reviewed have similar trends, from a relatively warm and wet stage to a cold and dry stage during Middle to Late Miocene; the only exception being the site closest to the Atlantic Ocean (Fig. 4W1), which doesn't show a cooling trend — possibly due to local/regional effects. Another site, near the Montes Alps, exhibits a conspicuously different precipitation development (Fig. 4W4), which can be explained by the strong influence of the Alpine uplift (Jiménez-Moreno et al., 2008). However this appears inconsistent with the explanation given by Bruch et al. (2006), which concludes there are no significant orographic effects linked to the Alps.

4.2. High latitude Asia (and Alaska)

Little scientific work focused on palynological studies in this large area covering West Siberia, NE Asia and Alaska. However the available results may be very important to understanding the climatic changes within higher latitudes from the Miocene to Pleistocene. Arkhipov et al. (2005) described the climate of West Siberia as warm-temperate and moderately wet during the Middle Miocene Climatic Optimum, and that it subsequently changed gradually toward cooler and dryer conditions. The Late Miocene (to Pleistocene) was then characterized by strongly increasing drought conditions, which can be summarized as the climate becoming more and more continental (Arkhipov et al., 2005; Fig. 5, at H1). Temperature trends of NE Asia (Fradkina et al., 2005; Fig. 5H2) closely resemble those from Siberia. The climate of this region changed to cooler and dryer conditions during the Miocene. White et al. (1997) analyzed palynological samples from eight different sites in Alaska (Fig. 5H3), and were able to reconstruct long term palaeoclimate trends in the region for the last 18 Ma. Their results indicate a warm and wet peak in Alaska around 15 Ma, followed by a steady temperature decline starting shortly afterwards, with a concurrent increase in precipitation (until ~8 Ma). After 8 Ma the precipitation steadily decreased until the Pleistocene. Climate became more continental, cold and dry. Recently, Popova et al. (2011) used the coexistence approach to reconstruct the climate development in Siberia and the Russian Far East based on a small number of fruit and seed floras. Their results document the transition from the Middle Miocene Climatic Optimum with warm and humid conditions to a cool temperate climate during the Pliocene.

4.3. East Asian Monsoon region

This study reviewed terrestrial studies of pollen, chemical weathering (CIA), and $\delta^{18}O$ studies on oceanic sediments in the East Asian Monsoon region. Korotky et al. (2005) analyzed palynological data from the southern Far East (Fig. 6E1), reconstructing the climate history between ~15 Ma and 5 Ma. Their study reconstructed climatic characteristics from three epochs (with the help of species-indicators from modern vegetation), and found evidence for a synchronous decrease of temperature and precipitation. Wang (1996) studied Neogene climate changes indicated in palynological samples from the Oga Peninsula (Japan) and the Himi Area of Central Japan. Their results reflect a general climate trend toward lower temperatures and drier conditions after the Middle Miocene Climatic Optimum (Fig. 6E2). Other studies from nearby regions such as the Pohang area, Korea (Chung and Koh, 2005) and the Yellow Sea Basin, Korea (Yi et al., 2003) have yielded similar results. In addition, a quantitative analysis of mean annual temperature based on leaf margin analysis revealed a clear trend of increasing mean annual temperatures during the Early Miocene in northeast Japan (Yabe, 2008), indicating a synchronous response of climate change to that on the Oga Peninsula

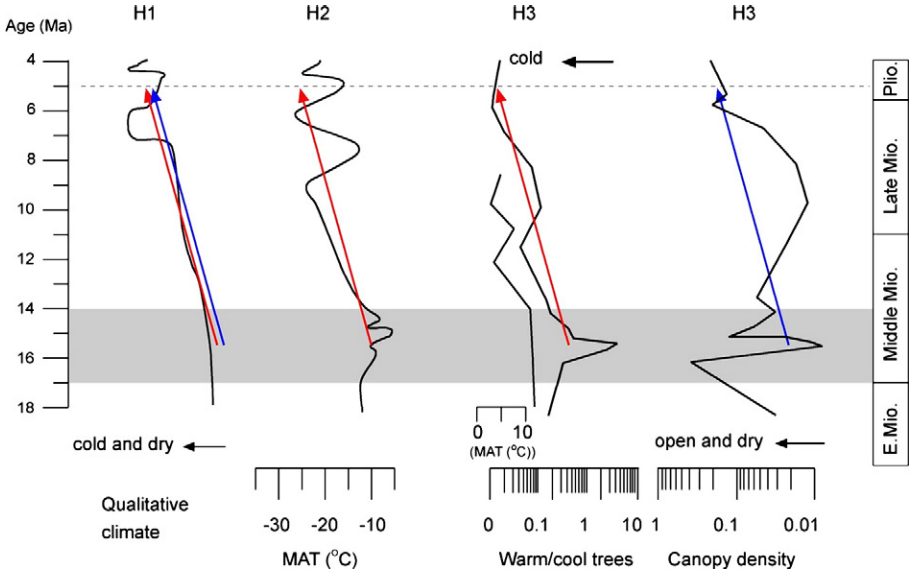

Fig. 5. Variations and long-term trends of High Latitude Asia (and Alaska) during the Mid-to-Late Miocene. Mean annual temperature (MAT) estimation at H3 (based on CLAMP; Wolfe, 1994). (Red arrows indicate temperature trends, blue arrows indicate aridity trends; The gray rectangle highlights the Middle Miocene Climatic Optimum).

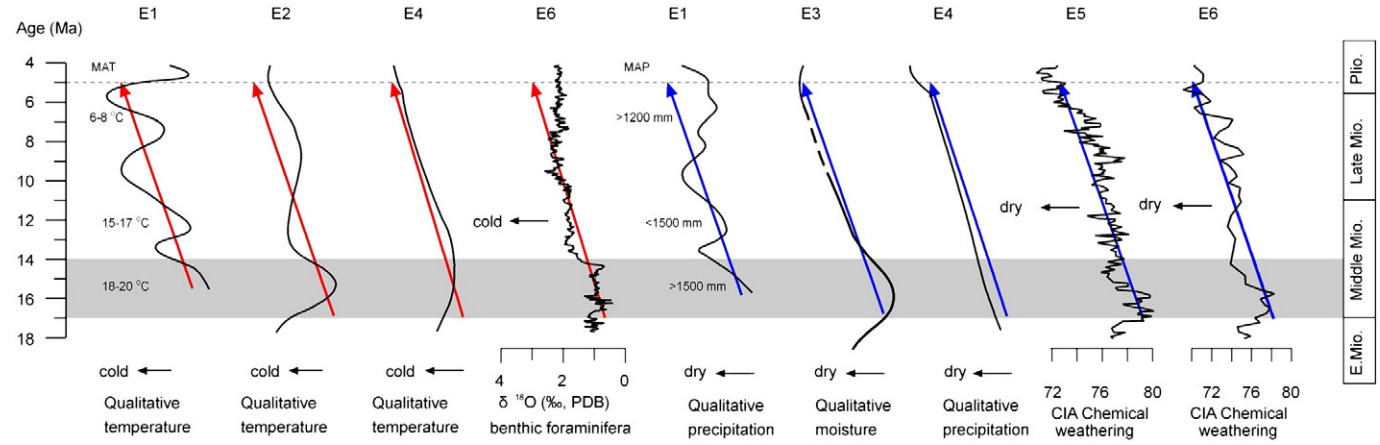

Fig. 6. Variations and trends in the East Asian climate during Mid–Late Miocene (red arrows indicate temperature trends, blue arrows indicate aridity trends). The gray rectangle indicates the Middle Miocene Climatic Optimum. Three quantitative climatic characteristics are named in diagrams E1 (after Korotky et al., 2005). MAT: mean annual temperature; MAP: mean annual precipitation, CIA: chemical index of alteration.

(Wang, 1996; Wang et al., 2001). Several pollen studies of the Shanwang Formation and other locations spanning the Miocene at Shandong Province, northern China revealed a general trend of climate degradation expressed as aridification during the Miocene (Fig. 6E3) (Wang, 1996). Relative temperature and precipitation trends reconstructed from pollen and spore analyses from Miocene age East China Sea samples (Hu and Sarjeant, 1992; Fig. 6E4) show trends similar to the results from the Oga Peninsula (Japan, see above). Pollen studies of samples from the Taibei Depression support these results (Li et al., 2003). Ocean Drilling Program (ODP) site 1146 in the South China Sea, provides a record of climate changes since 19.5 Ma (Wang et al., 2000). A series of geochemical proxies derived from major and trace element compositions (esp., Rb, Sr, and Ba) of siliciclastic sediments have been used to infer changes in the intensity of the East Asian summer monsoon. Fig. 6 (site E5) illustrates that the trends of the CIA values, used as a moisture index, vary almost synchronously with the global cooling indices (Wan et al., 2007; 2010). Similarly, high resolution oxygen isotope records on benthic foraminifers from ODP site 1148 in the South China Sea (Wang et al., 2003; Cheng et al., 2004), indicate decreasing seafloor temperatures since the Middle Miocene (Fig. 6E6). The CIA trend (Wei et al., 2006) at ODP site 1148 is similar and has been used to indicate the precipitation changes (Fig. 6E6) that are also supported by C_{RAT} (the mineralogical ratio chlorite/(chlorite + haematite + goethite)) records, another proxy used for changes in moisture (Clift, 2006; Clift et al., 2008).

4.4. South Asian Monsoon region

Three sites from the Himalayan foreland basin and two marine sites of the Arabian Sea provide an insight into the development of temperature and moisture during the Miocene in the South Asian Monsoon region. On the Potwar Plateau, Pakistan, the Siwalik Group contains mighty fluvial to lacustrine sediment sequences, spanning the past 18 Ma (Quade et al., 1989). Results of the $\delta^{18}O$ isotope analysis (Fig. 7S1) of pedogenic carbonates reveal the moisture evolution in the Himalayan foreland (Quade et al., 1989; 1995). Another study of $\delta^{18}O$ data (Fig. 7S2; Sanyal et al., 2004; 2005) from the Himalayan Foreland Basin of Northern India, spanning the past ~12–2 Ma, also provides information about the moisture evolution, showing similar trends of decreasing precipitation with time. Palynological studies (Hoorn et al., 2000; Ohja et al., 2000) at the Surai Khola Section, Central Nepal, spanning the time from ~11.5 to <2 Ma, yield information regarding changes in temperature and moisture (by using the percentages of tropical forest and grassland taxa), and indicate climatic cooling and drying (Fig. 7S3). CIA indices of the drill hole Indus Marine A-1 in the Arabian Sea, span the period between 17 and 3 Ma

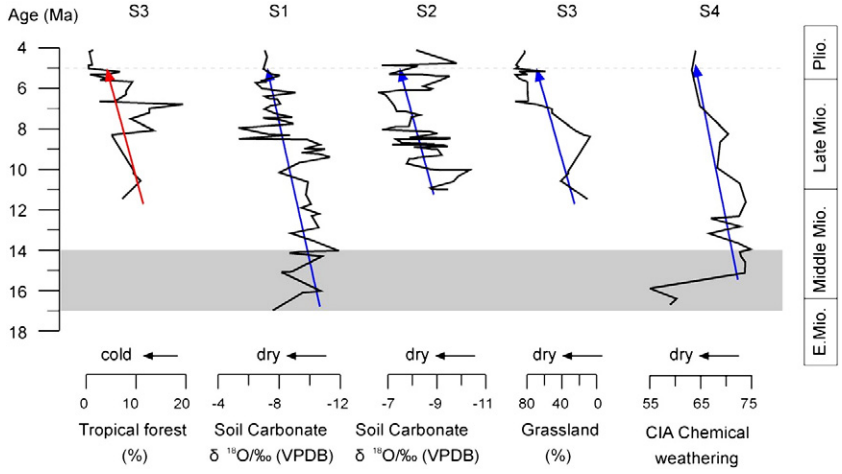

Fig. 7. Variations and trends in the South Asian climate during Miocene (red arrows indicate temperature trends, blue arrows indicate aridity trends; the gray rectangle indicates the Middle Miocene Climatic Optimum). CIA: chemical index of alteration.

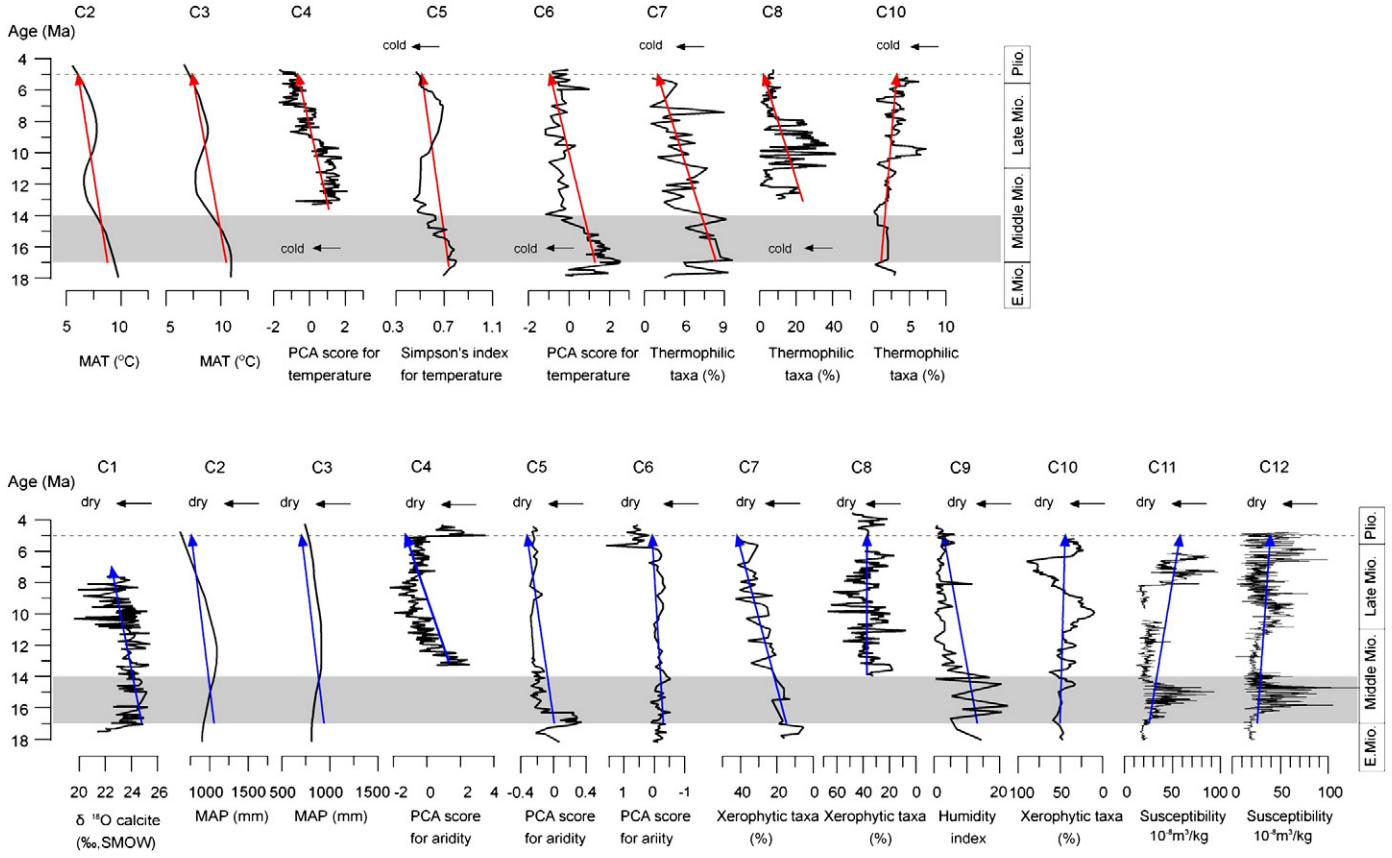

Fig. 8. Variations and trends of the Central Asian climate during Mid–Late Miocene (Upper part: temperature, lower part: precipitation). Red arrows indicate temperature trends, blue arrows indicate aridity trends; the gray rectangle identifies the Middle Miocene Climatic Optimum. MAT: mean annual temperature, MAP: mean annual precipitation.

ago, and indicate a drying period starting at about 15 Ma (Clift et al., 2008; Fig. 7S4), and show some similarity with the C_{RAT} and K/Al results from ODP Site 1148 (Fig. 6E6; see above).

4.5. Central Asia

Central Asia constitutes the core region of the Asian continent, spanning from the Caspian Sea in the west to China in the east, and from Afghanistan in the south to Siberia in the north. Our study complied data from a total of 12 different locations within this region to derive information about its Miocene climate change. Ballato et al. (2010) studied Miocene lacustrine and palustrine sediments (~17.5–7.6 Ma) from northern Iran for their stable oxygen isotopes and interpreted the results to reflect primarily precipitation changes, showing an increase in aridity (Fig. 8C1). Akhmetyev et al. (2005) analyzed Miocene palynological samples from northwest Kazakhstan (Fig. 8C2) and the Zaisanskaya depression (Fig. 8C3) that reflect increasing climate degradation (cooling and drying). The regional climate became more and more continental, showing increasing seasonality. Pollen analyses of three different sections determined to be of Miocene age (the Kuchetawu section (Fig. 8C4); the Jingouhe section (Fig. 8C5), and the Taxihe section (Fig. 8C6)) of the Tianshan Range provide somewhat different results. Zhang and Sun (2011) interpret their research to indicate a gradual cooling and drying trend at the Kuchetawu section (Fig. 8C4); and Tang et al. (2011) find the same at the Jingouhe section (Fig. 8C5). However, Sun and Zhang (2008) interpret samples from the Taxihe section to only reflect a similar trend in temperature, although they find that arid conditions remained essentially stable throughout the Mid–Late Miocene (Fig. 8C6). Miao et al. (2011a) suggest that the palynology of the KC-1 core, Qaidam Basin (Fig. 8C7; also see Section 3.2, Fig. 3a, b) reflects decreasing temperatures and increasing aridity within the Qaidam Basin. The Laojunmiao section (located in the Jiuquan Basin, north of Qaidam Basin) yields samples with ages of 13.0–2.2 Ma (Fang et al., 2004). Ma et al. (2005) find the sporopollen record of this section to reveal a long lasting cooling trend, but showing a slightly increasing trend of humidity (Fig. 8C8). Jiang and Ding (2008) describe palynological samples of the Sikouzi section, Ningxia Basin, spanning the time interval of 20.1–0.1 Ma, and find evidence for almost stable moisture conditions since 14 Ma and that temperature development there follows the global climate cooling (Fig. 8C9). Ma et al. (1998) carried out pollen analysis at samples of the Maogou section, Linxia Basin (Fig. 8C10). Magnetostratigraphic age control by Li et al. (1995) yielded a range of ages between 30.6 and 4.0 Ma. Results of temperature and precipitation reconstruction (Ma et al., 1998) deviate somewhat from the studies presented above (Fig. 8C1–9). Loess/red clay sediments from the Qin'an-I section, Tianshui Basin (Fig. 8C11) (Guo et al., 2002), and from the ZL-1 cores (southern margin of the Tenggeli Desert) (Fig. 8C12) (Qiang et al., 2011) reflect trends of moisture evolution based on the magnetic susceptibility data during Mid–Late Miocene. These indicate generally increasing precipitation rates, with two somewhat stronger peaks between 15 and 13 Ma and between 8 and 7 Ma, at both locations, and show a slight wetting trend between 17 and 5 Ma. Research at the Qin'an-I section by Liu et al. (2006) and Liang et al. (2009) provides additional information on geochemical characteristics, grain-size features, quartz morphology and quartz grain-size. Those data yield similar results with regard to climate development.

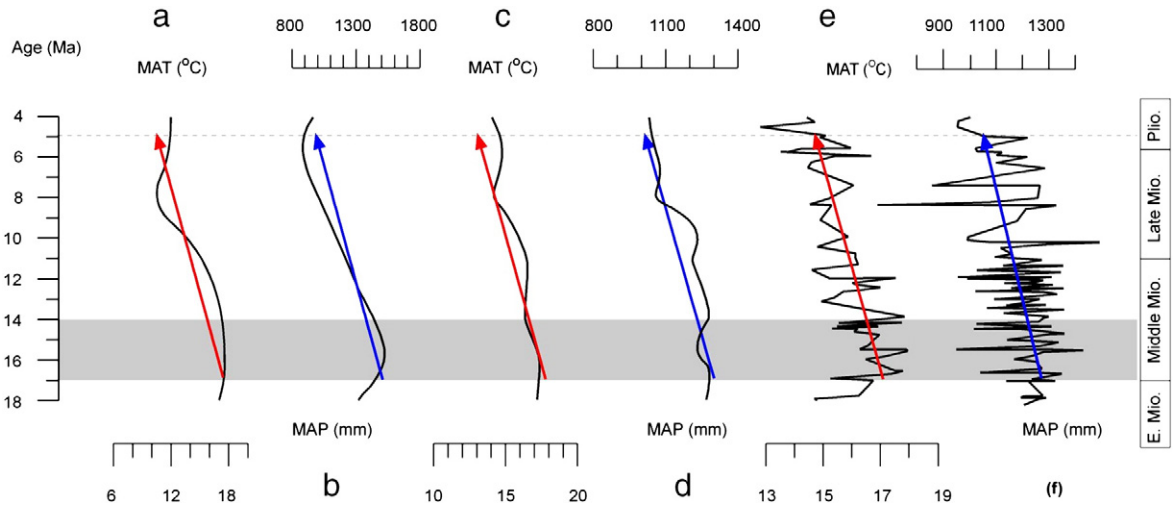

Fig. 9. Variation and trends of (a) mean annual temperature (MAT) and (b) mean annual precipitation (MAP) in Central Europe, based on palaeobotanical data (adapted from Bechtel et al., 2008). Trends of (c) MAT and (d) MAP from the Central and Eastern Paratethys (adapted from Ivanov et al., 2011), and the trends of compiled (e) MAT (average of Fig. 4, W1–W8) and (f) MAP (average of Fig. 4, W1–W10) from most of the reviewed European sites (this text).

5. Discussion

5.1. Common climatic trends of Eurasia

In addition to the Miocene climate in the European sites discussed above, other researchers have discussed temperature and precipitation patterns during this period on large spatial scales (e.g., Utescher et al., 2000; 2009; Mosbrugger et al., 2005; Bruch et al., 2006; van Dam, 2006; Bechtel et al., 2008; Böhme et al., 2011; Bruch et al., 2011; Ivanov et al., 2011; Liu et al., 2011). For example, Mosbrugger et al. (2005) summarized the climate records of the Lower Rhine Basin and the Weisselster Basin, finding the relationship between the mean annual temperature and mean annual precipitation to be ambiguous; whereas Bechtel et al. (2008) found good positive correlations between mean annual temperature and mean annual precipitation (Fig. 9a and b) in Central Europe (area of black line, Fig. 2). Ivanov et al. (2011) presented another feature during their research on Central and Eastern Paratethys floras (Serbia, Ukraine Carpathians and Ukraine Plain, Bulgaria, and northern Germany). They detected a good correspondence between the mean annual temperature and cooling of the oceans (as represented by Zachos et al., 2001) based on the marine oxygen isotope records. For this study, we compiled the quantitative temperature and precipitation data described above, and found the results to clearly show correlations between temperature and precipitation (Fig. 9c and d). Similarly, the mean annual precipitation trends, reconstructed by using small mammal communities in European locations during the late Neogene (12–3 Ma), exhibited a gradual decrease (van Dam, 2006). Neglecting the local influences mentioned by Böhme et al. (2011) and the differences in data resolution within the various studies, we conclude that the Miocene global cooling provided the controlling factor for precipitation in Europe. Fig. 9e, f shows the persistent trend of the climate change by compiling absolute values of mean annual temperature and precipitation at the European sites. The gradual cooling process all over Europe correlates well with falling deep-sea temperatures, and with decreasing precipitation rates in Europe during the Mid–Late Miocene (Fig. 9).

The High-latitude Asia sites discussed above (Fig. 5) dramatically reflect the global cooling trend, as provided by Zachos et al. (2001, 2008). Also, the trends found for the East Asian Monsoon sites show high degree of correspondence (Fig. 6), as do the South Asian Monsoon sites (Fig. 7). Based on the compiled climate graphs for the Asian sites surrounding Central Asia, the relative trends of the Miocene temperature and precipitation patterns on a large spatial scale appear consistent: the climates within all of these regions were warm and humid during the Middle Miocene and became continuously cooler and dryer thereafter. Eronen et al. (2010) used mammal ecomorphology on a Eurasian-wide scale to support these results. In Central Asia, however, this picture is not that clear. In Northern Iran (Fig. 8C1) (Ballato et al., 2010), Northwestern Kazakhstan (Fig. 8C2) (Akhmetyev et al., 2005), and the Zaisanskaya Basin (Fig. 8C3) (Akhmetyev et al., 2005), the curves show climate changes similar to Europe's. The Tianshan region (Kuchetawu section (Fig. 8C4) (Zhang and Sun, 2011), Jingouhe section (Fig. 8C5) (Tang et al., 2011) and Taxihe (Fig. 8C6) (Sun and Zhang, 2008) show a cooling trend, but with precipitation remaining relatively stable throughout the Miocene. Studies carried out on the Northeastern Tibetan Plateau, the KC-1 core, the Qaidam Basin (Fig. 8C7) (Miao et al., 2011a), and Sikouzi, Ningxia (Fig. 8C9) (Jiang and Ding, 2008) yield evidence of decreasing precipitation rates during the Miocene, whereas xerophytic taxa percentages in samples from Laojunmiao, Jiuquan Basin, (Fig. 8C8) (Ma et al., 2005) show significant fluctuations, but have an overall stable trend. Other investigated sites, however, including the Linxia Basin (Fig. 8C10) (Ma et al., 1998), Qin'an, Tianshui Basin (Fig. 8C11) (Guo et al., 2002), and the Zhuanglang Core (Fig. 9C12) (Qiang et al., 2011) show trends of increasing moisture with strong fluctuations. Central Asia appears to exhibit indeterminate relationships during this time period.

5.2. Influence of global cooling on Eurasian climate trends

Global climate conditions changed progressively from the Paleocene/Eocene greenhouse to Quaternary icehouse conditions. The Miocene appears a key period for understanding this cooling process, which includes a strong fluctuation in $\delta^{18}O$, from 2.8‰ to 1.8‰ during the Early Miocene (24–17 Ma), followed by the Middle Miocene Climatic Optimum (Flower and Kennett, 1994), with a mid-latitude warming to about 6 °C higher than present day temperatures. Following the Optimum, $\delta^{18}O$ steady increased at about 1.0‰ (between 2.2‰ and 3.2‰) during the Late Miocene (14–5 Ma), driven by the growth of the polar ice-sheets (e.g., Zachos et al., 2001; 2008).

Terrestrial deposits contain climatic information in addition to that stored in ocean sediments. Ruddiman (2002) discussed how the growth of the polar ice-sheets not only controls the oceanic water temperatures but also inland temperatures by way of the Earth's energy circulatory systems. Relative temperature trends in Europe (based on paleobotanical data) show a decrease between

17 Ma and 5 Ma (Fig. 9), which matches the temperature trends determined from the deep-sea isotope record, and long-term temperature trends from High latitude Asia (Fig. 5), the East Asian Monsoon region (Fig. 6), the South Asian Monsoon region (Fig. 7), and most sites in Central Asia (Fig. 8).

Water vapor also functions as a dominant greenhouse gas and provides a major feedback with the atmosphere. Higher temperatures produce higher concentrations of water vapor in the atmosphere, producing a significant positive feedback in the climate system (e.g., Singh, 1988; Ruddiman, 2002; Held and Soden, 2006). The Westerlies transport humid air from the Atlantic Ocean, which resulted in synchronous decreasing trends in precipitation and temperature during the Miocene. Cooling occurred under increasingly continental conditions, expressed by seasonality of temperature and precipitation (e.g., Bruch et al., 2011). This same process may explain the moisture evolution of High latitude Asia (Fig. 5), which is linked to the Arctic Ocean and/or to the North Pacific Ocean. Warmer episodes (ice-free/reduced stages) cause higher evaporation rates and hence bring more water vapor into the atmosphere than during colder episodes with strong ice coverage. In the East Asian Monsoon region (Fig. 6) and the South Asian Monsoon region (Fig. 7), effective precipitation directly controls the initiation and evolution of the monsoonal system (e.g., Liu et al., 1998; Guo et al., 2002; Sun and Wang, 2005), on which the corresponding air mass transport also plays a role (e.g., Jiang and Ding, 2008; Sun and Zhang, 2008; Passey et al., 2009; Tang et al., 2011; Zhang and Sun, 2011). Within these regions, the notable gradual decrease of precipitation can also be linked to the global cooling process (Figs. 6, 7).

All of the regions surrounding Central Asia show the same decreasing trends in water supply during the Mid–Late Miocene, driven by the global cooling (Figs. 4–7). Any moisture reaching Central Asia had to cross at least one of these surrounding regions. One would therefore expect precipitation rates to be stronger during 'warmer" stages than during the "colder" stages. And trends extracted from Central Asian sites should show tendencies similar to its surrounding regions (relatively high during Early–Mid Miocene then lowering during Late Miocene). Well-developed palaeosols in the Tianshui Basin document that higher amounts of moisture reached Central Asia during warmer stages (Guo et al., 2008), as do wet-tolerant mammal fossils in the Linxia Basin (Deng, 2009), and the lack of large areas of fine grained loess sediments in northwest China (Lu et al., 2010). Less precipitation at the end of the Miocene corresponds with falling temperatures, scattered pollen data (Liu et al., 2011), enrichment of gnawing animals in the Linxia Basin (Deng, 2009), and enlarged loess-covered areas with coarser grain sizes (Lu et al., 2010). However, our study shows that long-term trends do not correspond as well (Fig. 8C10). This suggests that another driving force contributes to the moisture evolution of Central Asia.

5.3. Influence of Tibetan Plateau uplift on Central Asian climate trends

Most of the climate histories of Central Asia (Fig. 8 and Fig. 10) contrast with precipitation trends in other Eurasian localities (Figs. 4–7). The uplift of the Tibetan Plateau (including the Tianshan Mountains) provides a possible explanation for the inconsistent precipitation trends of Central Asia. Many models support the conclusion that a rapid uplift of the Tibetan Plateau could have caused a strong drying of Inner Asia (e.g., Manabe and Terpstra, 1974; Kutzbach et al., 1989; Ruddiman and Kutzbach, 1989; Manabe and Broccoli, 1990; Raymo and Ruddiman, 1992; Liu et al., 2003; Zhang et al., 2007). This supports the ideas that orogenesis could effectively disturbed precipitation patterns in the mountainous regions while Central Asia (especially the Tibetan Plateau) underwent various extensive phases of orogeny. Mountain sites, especially windward of the mountains, can get high precipitation rates that contrast to those on the large plains of Eurasia in the lee of mountains, which mostly have drier conditions. For example, much of the area between the Caspian Sea and China (around 30°–50° North latitude and 50°–70° East longitude, and with relatively flat landscape) experience mean annual precipitations of less than 300 mm, whereas the area of the Tianshan Mountains (also considered the Northwestern Tibetan Plateau), the precipitation can reach more than 400 mm just because of topographic effects (Fig. 1).

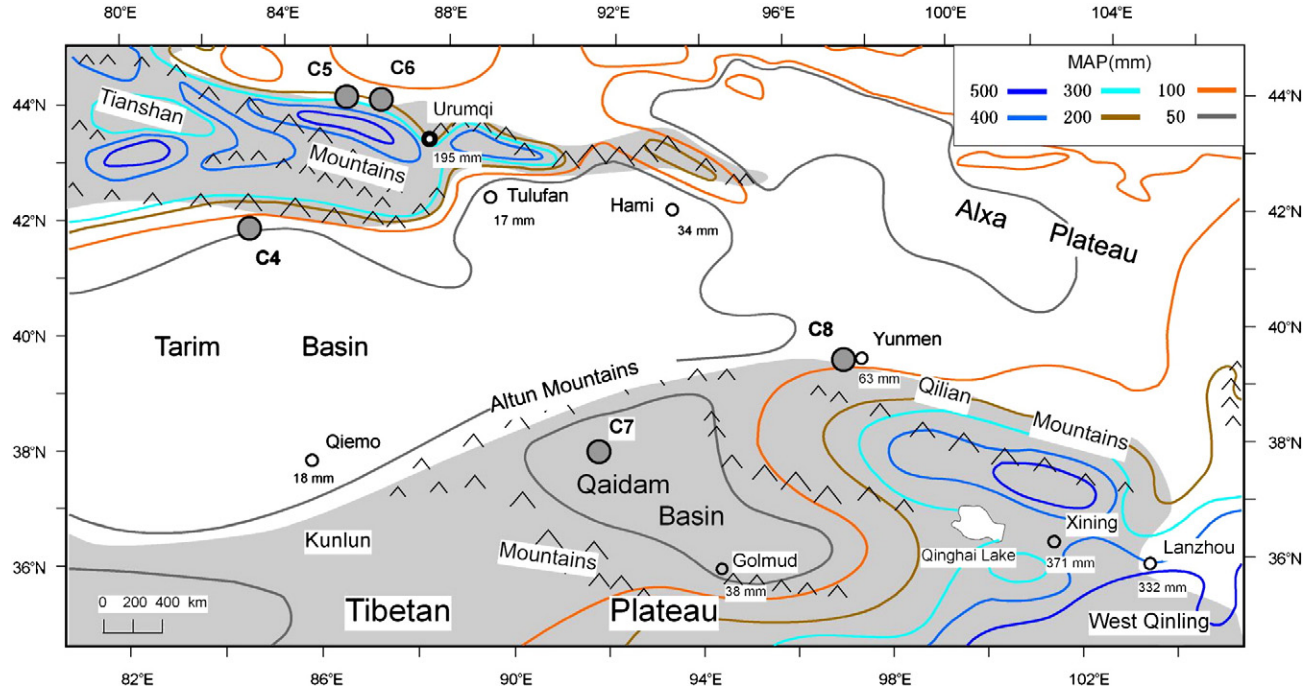

Fig. 10. The orographic rainfall on the North Tibetan Plateau and adjacent areas. High precipitation rates on the northwestern and northeastern Tibetan Plateau contrast with the low precipitation rates of the other investigated areas. C4: Kuchetawu section, Tianshan Range; C5: Jingouhe section, Tianshan Range; C6: Taxihe section, Tianshan Range; C7: KC-1 core, Qaidam Basin; C8: Laojunmiao section, Jiuquan Basin.

For example, great differences in precipitation occur over relatively short distances on the Northwestern Tibetan Plateau because of different topography and elevation (Fig. 10). The Tianshan Mountains receive more than 400 mm, whereas the nearby isolated leeward basins of Tulufan and Hami get only 17 mm and 34 mm respectively. A similar situation occurs in the Qilian Mountains, Northeastern Tibetan Plateau. Here zonal precipitation exceeds 400 mm, whereas isolated leeward area like Yumen only receives about 63 mm. The Qaidam Basin provides a third example: surrounded by the Qilian, Altun and Kunlun mountains, it receives less than 50 mm of annual precipitation (Fig. 10).

These observations demonstrate that "humid" areas of the Northwestern and Northeastern Tibetan Plateau contrast with the arid portions of Central Asia largely because of orographic rainfall shadows.

5.3.1. Northwestern Tibetan Plateau (Tianshan region)

Numerous studies document the tectonic uplift of the Tianshan region during the Miocene based on tectonic patterns, sediment research, paleobotanical analysis, etc. (e.g., Avouac et al., 1993; Hendrix et al., 1994; Yin et al., 1998; Burchfiel et al., 1999; Deng et al., 2000; Sun et al., 2004, 2007, 2009; Charreau et al., 2006; Huang et al., 2006; Sobel et al., 2006; Sun and Liu, 2006; Hubert-Ferrari et al., 2007; Sun and Zhang, 2009; Fu et al., 2010; Sun et al., 2011).

We argue that the uplift of the Tianshan Mountains changed precipitation patterns within this region, and played the key factor for why the Kuchetawu section (Fig. 8C4) (Zhang and Sun, 2011), Jingouhe section (Fig. 8C5) (Tang et al., 2011) and Taxihe (Fig. 8C6) (Sun and Zhang, 2008) near the Tianshan show roughly similar cooling trends, but received relative stable precipitation throughout the Miocene. In fact, Zhang and Sun (2011) present evidence from the Kuchetawu section that shows clearly that the uplift of the southern Tianshan Range occurred at ~7 Ma. At Jingouhe, regional mountain building between about 16.2–13.5 Ma most likely influenced climatic change of this region (Tang et al., 2011). An arid climate occurred at 6 Ma in the Taxihe section (Fig. 8C6), and this corresponds with climatic worsening, recorded at higher latitudes of the Northern Hemisphere (Sun and Zhang, 2008) and an uplift at around 7 Ma (Sun et al., 2007). A relative wide area of the Tianshan Range, the Kuitun He section (~50 km to the west of Jingouhe section) shows an active uplift at ~10.5 Ma (Charreau et al., 2005). In summary, although difficulties persist in estimating absolute elevations reached by the various uplift events for these separated locations, and spatial and temporal data remain incomplete, variable, and sometimes contradictory, we conclude that the uplift of the Tianshan Range strongly influenced moisture development on the Northwestern Tibetan Plateau. A unique regional precipitation pattern evolved.

5.3.2. Northeastern Tibetan Plateau

The Miocene locations that have been analyzed (Fig. 8C7–12) show different trends in precipitation history. The first two locations (sites C7 and C9, Fig. 8) show drying trends, whereas samples from sites C10–C12 (Fig. 8) record wetting trends.

The lithofacies (from stable and continuous lacustrine environments) from the KC-1 core (Fig. 3; Fig. 8, C7), and pollen from the same core (counts and taxa of each sample remaining stable) may indicate that no major uplift of the basin or the surrounding mountains took place between 18 and 5 Ma (Miao et al., 2011a). The only faulting detected close to the KC-1 location occurred in the eastern basin, about 400 km away (Fang et al., 2007; Lu and Xiong, 2009). However, some tectonic events occurred in the North Qilian Shan (Bovet et al., 2009) and the Altun Mountains (Ritts et al., 2008) during this time.

The Laojunmiao section (Fig. 8C8), shows evidence of strong tectonic uplift of the Qilianshan Mountains at about 8.3–5.0 Ma, i.e.,

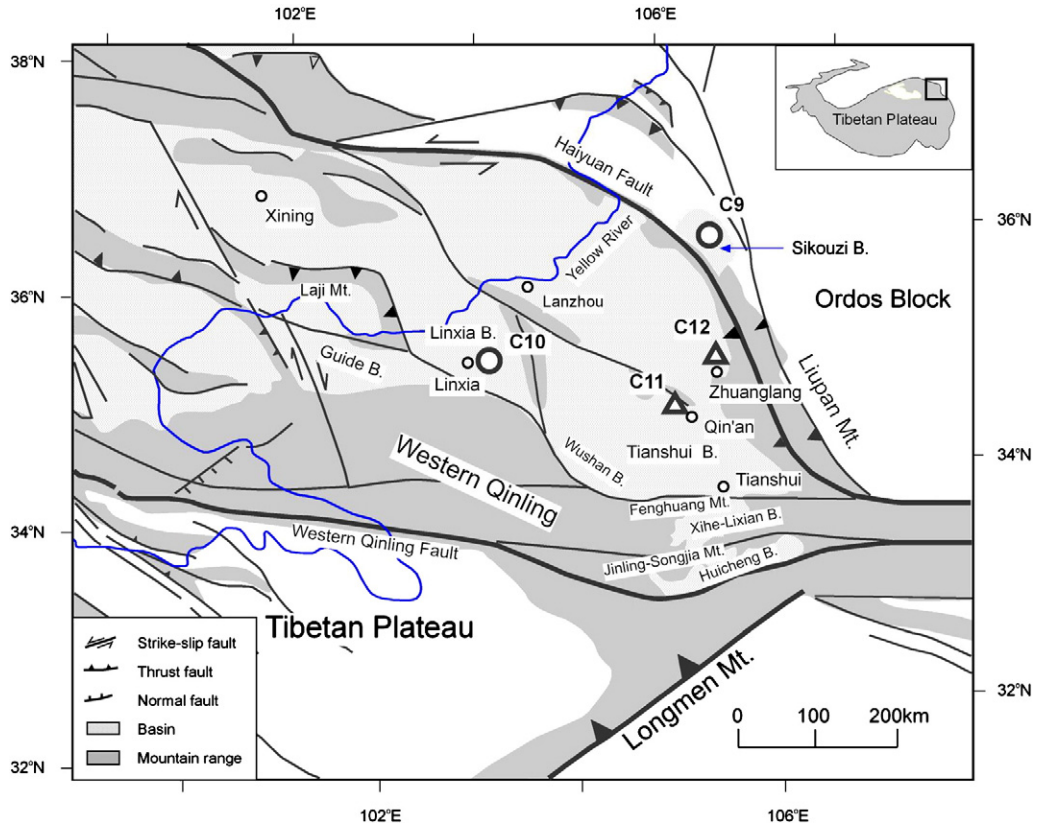

Fig. 11. Geological map of the northeasternmost Tibetan Plateau, showing locations of sites reviewed in detail (modified after Fang et al. (2005) and Wang et al. (2011b). C10: Maogou section, Linxia Basin; C11: Qin'an section, Tianshui Basin; C12: ZL cores, Zhuanglang; B.: Basin).

increasing gravel content and component size, changes in bedding dips and source rock types, and marginal growth faults (Song et al., 2001a). After this tectonic event, the percentages of xerophytic taxa diminished (Fig. 8C8) (Ma et al., 2005), indicating an increase in precipitation.

Based on pollen data from the Sikouzi section (Fig. 8C9; location also shown in Fig. 11), the East-Asian summer monsoon was generally strong between 20.1 and 14.2 Ma, decreased between 14.2 and 11.3 Ma, and has been weaker since 11.3 Ma (Jiang and Ding, 2008). Grain-size data support the palynological results (Jiang and Ding, 2010). Zheng et al. (2006) and Lin et al. (2010) detected a series of tectonic uplift events in this region by the apatite fission-track data, with ages between ~9.5 Ma and 8.2–7.3 Ma. Wang et al. (2011a) report uplift at ~10.5 Ma and Song et al. (2001b) at about 8.0 Ma, from sediment analyses. Those surface uplift events influenced the monsoon intensity, but may not have provided the controlling factor. Some fluctuations occur in the pollen data (Jiang and Ding, 2008) and grain-size data (Jiang and Ding, 2010) that correspond to those tectonic events, but no changes within the major climate trend became obvious (Fig. 8C9).

Precipitation rates in the Linxia Basin (Fig. 8C10; location also shown in Fig. 11) remained relatively stable, but did show strong fluctuations on longer time scales, especially after 12 Ma (Fig. 8C10; location also shown in Fig. 11). Contemporary sediments from around 12 Ma from the Heilinding section (about 30 km to the south of the Maogou section) unconformable cover the Caledonian granite (Wang et al., 2010), and at ~6 Ma, Fang et al. (2003) exhibit a 10° clockwise rotation at the Maogou section in the central Linxia Basin. Decreasing percentages of the xerophytic taxa document these two events. Both events mark periods of increasing monsoonal intensity, causing higher rainfall rates (Fig. 8C10). Loess deposits at Qin'an (Fig. 8C11), and the Zhuanglang Cores (Fig. 8C12) show changes of the magnetic susceptibility that indicate wetting trends (e.g., Guo et al., 2002; Qiang et al., 2011). Heller and Liu (1982, 1984), Liu (1986), Kukla et al. (1988), An et al. (1991; 2000) and Vandenberghe et al. (2004), for example, have successfully applied this method on loess and red-clay sediments from other parts of the Loess Plateau, Northwest China. We think that the higher rainfall rates were controlled by the uplift of the mountains around them, rather than by a strengthening of the Asian monsoon. We do not believe that global cooling alone could have provided sufficient water vapor at these two sites to account for the decrease in the atmosphere after ~14 Ma (see detailed explanation in Section 5.4). Alternatively, those wetting trends (see above, Fig. 8C11–12) could have resulted from an intensification of the summer monsoon. But this would contradict to the observed relationships between pollen data, grain-size data, and the monsoonal system (Jiang and Ding, 2008; Jiang and Ding, 2010), or to the pollen results from the Tianshui Basin (Hui et al., 2011). Therefore, there remains the assumption that the wetting trends could have been controlled by the uplift of the mountains around them. The topographic changes strengthened precipitation rates on windward slopes and decreased the precipitation on leeward slopes. Susceptibility increased linked to higher precipitation rates caused by the mountain uplift. Wang et al. (2011c) reported a major deformation at ~16 Ma in the Wushan Basin based on their magnetostratigraphic study; Li et al. (2006) and Hou et al. (2011) identified an uplift event at ~8.0–6.0 Ma in the Tianshui Basin might have documented an increase of the magnetic susceptibility at ~16 Ma and ~8 Ma respectively (Fig. 8C11 and C12).

In order to illustrate the relationships between the uplift and the precipitation history, we have redrawn a cartoon picture from Wang et al. (2011b; Fig. 12a, b). During the Early Miocene, the Northeastern Tibetan Plateau actively deformed with intense surface uplift occurring near the Western Qinling Mountains; the orographic rainfall fell most near the Western Qinliang due to the topographic effect. In the large Huicheng–Tianshui Basin, however, the climate remained

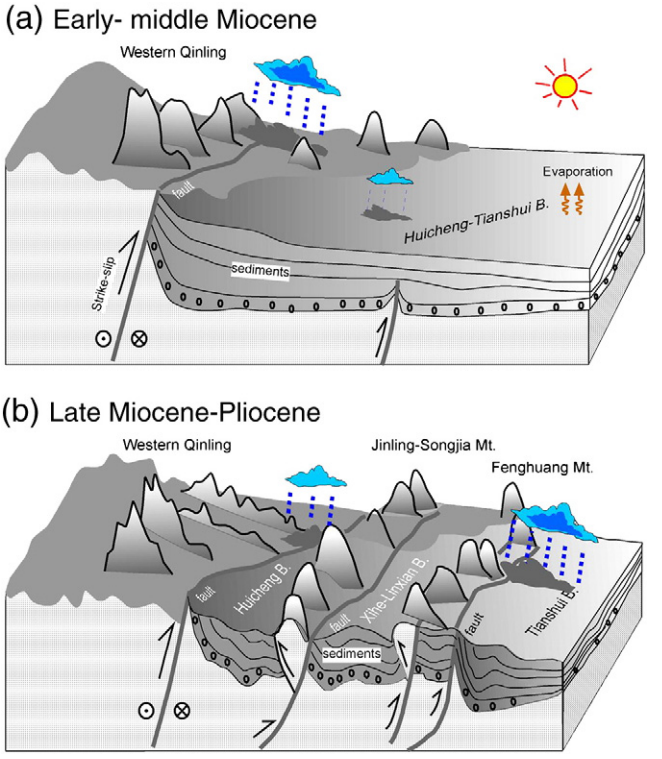

Fig. 12. Cartoons illustrating the tectonic and topographic evolution of the Tianshui region from Early Miocene to the Pliocene that influenced the rainfall patterns (after Wang et al., 2011b).

relatively dry due to strong evaporation compared to the precipitation (Fig. 12a). During the Late Miocene after a series of tectonic uplifts, the basin was separated into the Tianshui, Xihe-Lixian, and Huicheng sub-basins by the Jinling-Songjia Mountains and the Fenghuang Mountains, respectively, after which more rainfall reached the smaller Tianshui Basin, and the climate became wetter (Fig. 12b).

Uplift of the Plateau can also help explain the climatic history documented in the KC-1 core, from the Qaidam Basin. The climate became dryer throughout the entire Miocene, not only because of the global cooling but also due to mountain uplift events (although some far from the basin). The mountains functioned as barriers, reducing the amount of water vapor carried to the Qaidam Basin by the Westerlies and the Asian monsoon. Overall, the influence of the tectonic uplifts within the Northwestern and Northeastern Tibetan Plateau, rather than the global cooling, strongly affected the precipitation patterns of these two regions (Fig. 13). Hence, the uplift of the North Tibetan Plateau caused the decisive influence for the climate change in these nearby regions.

In fact, much additional evidence exists for a strong uplift in or around the Tibetan Plateau during the Miocene. This evidence includes: (1) tectonic patterns (e.g., Yin et al., 1994; Hodges et al., 1996; Chemenda et al., 2000; Bovet et al., 2009), (2) volcanic activity (e.g., Leloup et al., 1995; Deng, 1998; Ding et al., 2003), (3) uplift of mountains (e.g., George et al., 2001; Coutand et al., 2002; Lu et al., 2004), (4) sedimentary changes (e.g., Chemenda et al., 2000; Jin et al., 2003; Fang et al., 2007; Lu and Xiong, 2009), (5) oxygen isotopes (e.g., Currie et al., 2005; Rowley and Currie, 2006; Wang et al., 2006; Decelles et al., 2007; Quade et al., 2011), and (6) paleobotanical analyses (e.g., Xu, 1978; Spicer et al., 2003; Song et al., 2010; Miao et al., 2011b).

Every uplift event, although different in space and time, could have changed the local precipitation patterns because of topographic effects. Overall, it is not possible to isolate any clear trend of precipitation on the Tibetan Plateau. The signal of global cooling combined

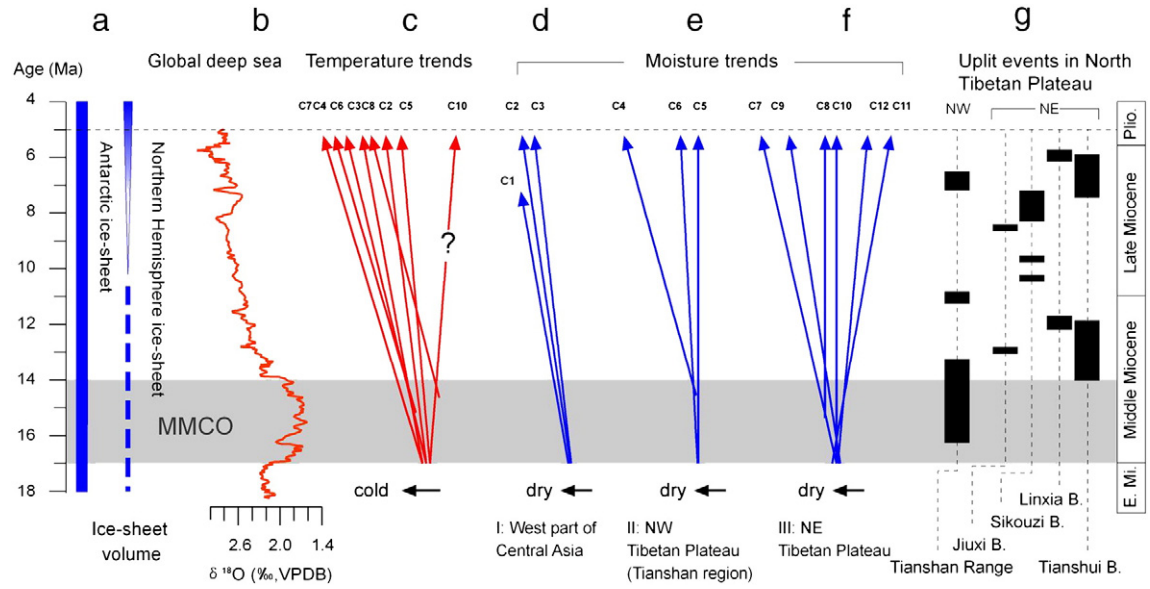

Fig. 13. Comparison of (a) the Miocene global ice-sheet development and (b) the global deep sea $\delta^{18}O$-isotope curve after Zachos et al. (2008), with (c) the temperature and (d, e and f) precipitation trends of Central Asia (d) (C1: North Iran; C2: North and west Kazakhstan; C3: Zaisanskaya Basin; C4: Kuchetawu, Tianshan Range; C5: Jingouhe, Tianshan Range; C6: Taxihe, Tianshan Range; C7: KC-1, Qaidam Basin; C8: Laojunmiao, Jiuquan Basin; C9: Sikouzi, Ningxia; C10: Maogou, Linxia Basin; C11: Qin'an, Tianshui Basin; C12: ZL, Zhuanglang). Uplift events of different basins (g) on the Northern Tibetan Plateau (the Tianshan Range after Charreau et al., 2005; Sun et al., 2007; Sun and Zhang, 2008; Tang et al., 2011; Zhang and Sun, 2011; the Jiuxi Basin after Song et al., 2001a; Sikouzi Basin after Song et al., 2001b; Zheng et al., 2006; Lin et al., 2010; Wang et al., 2011a; Linxia Basin after Fang et al., 2003; Wang et al., 2010; and the Tianshui Basin after Li et al., 2006; Hou et al., 2011; Wang et al., 2011b).

with tectonic effects lead to unusual regional and local patterns of precipitation histories within Central Asia opposite to those of the surrounding regions.

5.4. Influence of the Asian monsoon, Paratethys, and other factors on Central Asian climate trends

Regardless of global cooling and Tibetan uplift, the Asian monsoon is considered the main precipitation resource for southern and eastern China and the eastern part of Central Asia (Fig. 1). However, over the long-term, the elevation of the Tibetan Plateau controls the Asian monsoon itself (e.g., Manabe and Terpstra, 1974; Kutzbach et al., 1989; Manabe and Broccoli, 1990; Raymo and Ruddiman, 1992; Liu et al., 2003; Zhang et al., 2007; Clift and Plumb, 2008; Micheels et al., 2011), and perhaps even the global cooling (e.g., Dupont-Nivet et al., 2007; Jiang and Ding, 2008; Sun and Zhang, 2008; Passey et al., 2009; Miao et al., 2011a; Tang et al., 2011; Zhang and Sun, 2011). Based on stable isotopes of soil carbonates (e.g., Currie et al., 2005; Rowley and Currie, 2006; DeCelles et al., 2007), the recent scientific consensus appears to favor a gradual growth and spreading of the Plateau since the onset of the continental plate collision in the Eocene. Indeed, deposits of Late Eocene age at Xoh Xil (for example; Quade et al., 2011) indicate that paleoelevations at that time were closer to the current elevations than previously thought (≤~2 km high, Cyr et al., 2005). Harris (2006) and Rowley and Garzione (2007) summarized the elevation history of the Himalayas and the southern, central, and northern Tibetan Plateau. They show that on the main part of the Tibetan Plateau, the elevation could have reached ≥~4 km before Early Miocene. The Miocene tectonic uplift after ~20 Ma might have occurred under the background of an already large and high-altitude plateau that mainly affected the northeastern part (e.g., Rowley and Currie, 2006; DeCelles et al., 2007; Rowley and Garzione, 2007; Quade et al., 2011). If this is correct, the relatively high stability of the Tibetan Plateau elevation (≥~4 km) during the Miocene only had a moderately stable influence on the Asian monsoon development, a conclusion also supported by general circulation models (e.g., Kutzbach et al., 1989; Ruddiman and Kutzbach, 1989; Liu et al., 2003; Zhang et al., 2007; Micheels et al., 2011). In other words, no evidence exists for relationships between the strength of the Asian monsoon and the Miocene uplift of the Tibetan Plateau, in that Tibet reached a crucial threshold allowing the monsoon to intensify, starting in the Early Miocene. Consequently, we see the role of the global cooling as one key factor for the monsoonal evolution during the Mid–Late Miocene, after the onset of the strong monsoonal system during the Early Miocene. In fact, climate curves from the East Asian Monsoon region and the South Asian Monsoon region show a weakening of precipitation along with the development of global cooling (Fig. 6, Fig. 7). Isotopic evidence from fossil mammals and soil carbonates in northern China during the Late Miocene and Pliocene support this connection (Passey et al., 2009).

The Cenozoic retreat of the Paratethys provided another key factor for the development of Central Asia's precipitation history. Ramstein et al. (1997) pointed out that the Paratethys retreat intensified the South Asian Monsoon and shifted the Central Asian climate from temperate to continental conditions, and may have played a role as important as the Tibetan Plateau uplift in driving the Asian monsoon. Fluteau et al. (1999) suggested that the shrinkage of the Paratethys Sea changed the large-scale atmospheric circulation. Hence, both the Sea shrinkage and the uplift contributed a major ways to the monsoon changes. Detailed experiments carried out by Zhang et al. (2007) confirmed that the Paratethys retreat could strengthen the East Asian Monsoon and greatly increase humidity in the monsoon areas and aridity in Central Asia. Moreover, Zhang et al. (2007) found the retreat of the Paratethys Sea to the Turan Plate (the western boundary lies at about 70–80° east longitude) to be the key control for the pattern of paleoenvironmental transitions in East Asia.

However, beginning in the Oligocene, the combination of a drop in sea level and tectonic uplift resulted in a large regression of the sea (e.g., Báldi, 1980; Rögl and Steininger, 1983; Rögl, 1998, 1999; Schulz et al., 2005). As a result, the Turan plate became part of the mainland in the Early Miocene (Rögl, 1998; Zhang et al., 2007). Later in the Miocene, the Paratethys retreated more gradually (Rögl and Steininger, 1983; Rögl, 1998), until a rapid shrinkage during the Messinian Salinity Crisis, which was characterized by inland seas completely separated from each other, leading to Inner Asia's current geography (Krijgsman et al., 1996; Popova et al., 2004). The most

important side-effects of the Paratethys development on the Asian climate occurred during the Late Oligocene to Early Miocene, when the monsoonal climate system intensified in Eastern Asia (e.g., Liu and Guo, 1997; Sun and Wang, 2005; Zhang and Guo, 2005). Moreover, with the closing of the Paratethys, Zhang et al. (2007) reasoned that Central Asia should become drier and the precipitation should significantly decrease. However the moisture curves do not show any such drying trends (Fig. 8), which means that the influence of the Paratethys was only of minor importance for Inner Asia's climate. The main driving factors must have been the global cooling and/or the uplift of the Tibetan Plateau.

Moreover, attention should be paid to the warming trend in the Linxia Basin (Fig. 7). The trend here goes contrary to the general global cooling trend, the pollen results from the neighboring Tianshui Basin (Hui et al., 2011), and various temperature proxy results (e.g., KC-1 core, Miao et al., 2011a). The exact reason for these responses remains unknown. Hopefully, future palynological studies on the Linxia Basin pollen samples will shed further light on this question.

Although in this paper we argue that global cooling might have controlled the precipitation history of Europe, High-latitude Asia, the South Asian Monsoon region, and the East Asian Monsoon region, we recognize that this empirical relationship between humidity/precipitation and temperature (derived from various heterogeneous records as an overall trend by integrating over a considerable timespan) may not have existed in all regional climate systems or over all time-intervals (see Section 5.3).

6. Summary and conclusions

This paper synthesizes the Mid–Late Miocene climate history (mainly from ~17 to 5 Ma), as presented by the reviewed publications out of different Eurasian regions (Europe, High-latitude Asia, East Asian Monsoon region, South Asian Monsoon region, and Central Asia) in order to examine the controlling factors for the aridification of Central Asia during Miocene times. We found synchronous decreasing trends of temperature and precipitation in the first four regions that show consistency with the oceanic oxygen isotope records. Global cooling appears to have been the key controlling factor behind the large scale moisture evolution of these first four regions during this time period. A plausible explanation maintains that global cooling reduced the amount of water vapor held in the atmosphere. In Central Asia, however, the precipitation patterns show different trends, which can be explained by the uplift of the Tibetan Plateau under the predominant global cooling climate. Mountain uplift at different times and magnitudes locally influenced the moisture evolution (such as local rain shadows) causing various moisture signals throughout Central Asia. The timing and amplitude of the Tibetan Plateau uplift during the Miocene need to be investigated in more detail in order to better understand the extent to which global cooling, uplift of the Tibetan Plateau, or even other yet undetected teleconnections influenced the drying of Central Asia. Future work on this topic should also re-address the quality and reliability of proxy data, especially from Inner Asia, to better understand the mechanisms of aridification.

Acknowledgments

This work is supported by the (973) National Basic Research Program of China (Grant No. 2011CB403000, 2010CB833401), the National Natural Science Foundation (NSFC grant nos. 41172153, 41002050, 40802041, 41071130, 41021001, 40920114001, 40902015), and the Foundation for Excellent Youth Scholars of CAREERI, CAS (51Y184991). We thank Prof. Fang Xiaomin, Song Chunhui, and Prof. Bill Isherwood for giving suggestions, plus Torsten Utescher and an anonymous reviewer.

References

Akgün, F., Kayseri, M.S., Akkiraz, M.S., 2007. Paleoclimatic evolution and vegetational changes during the Late Oligocene–Miocene period in Western and Central Anatolia, Turkey. Palaeogeography, Palaeoclimatology, Palaeoecology 253 (1–2), 56–90.
Akhmetyev, M.A., Dodoniv, A.E., Somikova, M.V., Spasskaya, I.I., Kremenetsky, K.V., Klimanov, V.A., 2005. Kazakhstan and central Asia plains and foothills. In: Velichko, A.A., Nechaev, V.P. (Eds.), Cenozoic Climate and Environmental Changes in Russia: Special Paper — Geological Society of America, 382, pp. 139–161.
Akkiraz, M.S., Akgün, F., Utescher, T., Bruch, A.A., Mosbrugger, V., 2011. Precipitation gradients during the Miocene in Western and Central Turkey as quantified from pollen data. Palaeogeography, Palaeoclimatology, Palaeoecology 304, 276–290.
An, Z.S., 2000. The history and variability of the East Asian paleomonsoon climate. Quaternary Science Reviews 19 (1–5), 171–187.
An, Z.S., Kukla, G., Porter, S.C., Xiao, J.L., 1991. Magnetic susceptibility evidence of monsoon variation on the Loess Plateau of Central China during the last 130,000 years. Quaternary Research 36, 29–36.
An, Z.S., Kutzbach, J.E., Prell, W.L., Porter, S.C., 2001. Evolution of Asian monsoons and phased uplift of the Himalaya–Tibetan plateau since Late Miocene times. Nature 411, 62–66.
Arkhipov, S.A., Volkova, V.S., Zolnikov, I.D., Zykina, V.S., Krukover, A.A., Kulkova, L.A., 2005. (Chapter 4: West Siberia) In: Velichko, A.A., Nechaev, V.P. (Eds.), Cenozoic Climate and Environmental Changes in Russia: Special Paper — Geological Society of America, 382, pp. 67–88.
Avouac, J.P., Tapponnier, P., Bai, M., Hou, Y., Wang, G., 1993. Active thrusting and folding along the northeastern Tienshan, and rotation of Tarim relative to Dzungaria and Kazakhstan. Journal of Geophysical Research 98, 6755–6804.
Báldi, T., 1980. The early history of the Paratethys. Bulletin of Hungarian Geological Society 110, 456–472.
Ballato, P., Mulch, A., Landgraf, A., Strecker, M.R., Dalconi, M.C., Friedrich, A., Tabatabaei, S.H., 2010. Middle to late Miocene Middle Eastern climate from stable oxygen and carbon isotope data, southern Alborz mountains, N Iran. Earth and Planetary Science Letters 300, 125–138.
Barrón, E., Rivas-Carballo, R., Postigo Mijarra, J.M., Alcalde Olivares, C., Vieira, M., Castro, L., Pais, J., Valle-Hernández, M., 2010. The Cenozoic vegetation of the Iberian Peninsula: a synthesis. Review of Palaeobotany and Palynology 162 (3), 382–402.
Bechtel, A., Gratzer, R., Sachsenhofer, R.F., Gusterhuber, J., Lücke, A., Püttmann, W., 2008. Biomarker and carbon isotope variation in coal and fossil wood of Central Europe through the Cenozoic. Palaeogeography, Palaeoclimatology, Palaeoecology 262 (3–4), 166–175.
Berggren, W.A., Kent, D.V., Swisher, C.C., Aubry, M.P., 1995. A revised Cenozoic geochronology and chronostratigraphy. SEPM. Special Publication 54, 129–212.
Böhme, M., Winklhofer, M., Ilg, A., 2011. Miocene precipitation in Europe: temporal trends and spatial gradients. Palaeogeography, Palaeoclimatology, Palaeoecology 304, 212–218.
Bovet, P.M., Ritts, B.D., Gehrels, G.G., Abbink, O.A., Darby, B.J., Hourigan, J., 2009. Evidence of Miocene crustal shortening in the North Qilian Shan from Cenozoic stratigraphy of the Western Hexi Corridor. American Journal of Science 309, 290–329.
Bruch, A.A., Utescher, T., Mosbrugger, V., Gabrielyan, I., Ivanov, D.A., 2006. Late Miocene climate in the circum-Alpine realm — a quantitative analysis of terrestrial palaeofloras. Palaeogeography, Palaeoclimatology, Palaeoecology 238, 270–280.
Bruch, A.A., Utescher, T., Mosbrugger, V., NECLIME members, 2011. Precipitation patterns in the Miocene of Central Europe and the development of continentality. Palaeogeography, Palaeoclimatology, Palaeoecology 304 (3–4), 202–211.
Burchfiel, B.C., Brown, E.T., Deng, Q.D., Feng, X.Y., Li, J., Molnar, P., Shi, J.B., Wu, Z.M., You, H.C., 1999. Crustal shortening on the margins of the Tien Shan, Xinjiang, China. International Geology Review 41, 665–700.
Charreau, J., Chen, Y., Gilder, S., Dominguez, S., Avouac, J.P., Sen, S., Sun, D.J., Li, Y.G., Wang, W.M., 2005. Magnetostratigraphy and rock magnetism of the Neogene Kuitun He section, northwest China: implications for Late Cenozoic uplift of the Tianshan mountains. Earth and Planetary Science Letters 230 (1–2), 177–192.
Charreau, J., Gilder, S., Chen, Y., Dominguez, S., Avouac, J.P., Sen, S., Jolivet, M., Li, Y., Wang, W., 2006. Magnetostratigraphy of the Yaha section, Tarim Basin, China: 11 Ma acceleration in erosion and uplift of the Tian Shan mountains. Geology 34, 181–184.
Chemenda, A., Burg, J.P., Mattauer, M., 2000. Evolutionary model of the Himalaya–Tibet system: geopoem based on modelling, geological and geophysical data. Earth and Planetary Science Letters 174 (3–4), 397–409.
Chen, M.Y., Hao, W.G., Yao, Y.Y., Shao, M.Y., 1990. On the relationship between the Antarctic ice sheet and the eolian deposit in China. Quaternary Sciences 3, 261–271 (in Chinese).
Cheng, X.R., Zhao, Q.H., Wang, J.L., Jian, Z.M., Xia, P.F., Huang, B.Q., Fang, D.Y., Xu, J., Zhou, Z., Wang, P.X., 2004. Data report: stable isotopes from sites 1147 and 1148. In: Prell, W.L., et al. (Ed.), Proceedings of the Ocean Drilling Program: Scientific Results, 184, pp. 1–12.
Chung, C.H., Koh, T.Y., 2005. Palynostratigraphic and palaeoclimatic investigations on the Miocene deposits in the Pohang area, South Korea. Review of Palaeobotany and Palynology 135, 1–11.
Clift, P.D., 2006. Controls on the erosion of Cenozoic Asia and the flux of clastic sediment to the ocean. Earth and Planetary Science Letters 241, 571–580.
Clift, P.D., Plumb, R.A., 2008. Massachusetts Institute of Technology, USA. The Asian Monsoon: Causes, History and Effects. Cambridge University Press, Cambridge.
Clift, P.D., Hodges, K.V., Heslop, D., Hannigan, R., Long, H.V., Calves, G., 2008. Correlation of Himalayan exhumation rates and Asian monsoon intensity. Nature Geoscience 1, 875–880.

Coutand, L., Strecker, M.R., Arowsmith, J.R., Hilley, G., Thiede, R.C., Korjenkov, A., Omuraliev, M., 2002. Late Cenozoic tectonic development of the intramontane Alai Valley, Pamir-Tien Shan region, Central Asia: an example of intracontinental deformation due to the Indo–Eurasia collision. Tectonics 21 (6), 1053.
Currie, B.S., Rowley, D.B., Tabor, N.J., 2005. Middle Miocene paleoaltimetry of southern Tibet: implications for the role of mantle thickening and delamination in the Himalayan orogen. Geology 33, 181–184.
Cyr, A., Currie, B.S., Rowley, D.B., 2005. Geochemical and stable isotopic evaluation of Fenghuoshan Group lacustrine carbonates, north-central Tibet: implications for the paleoaltimetry of Late Eocene Tibetan Plateau. Journal of Geology 113, 517–533.
DeCelles, P.G., Quade, J., Kapp, P., Fan, M.J., Dettman, D.L., Ding, L., 2007. High and dry in central Tibet during the Late Oligocene. Earth and Planetary Science Letters 253, 389–401.
Deng, W.M., 1998. Cenozoic Intraplate Volcanic Rock in the Northern Qinghai-Xizang Plateau. Geological Publishing House, Beijing, pp. 1–180 (in Chinese).
Deng, T., 2009. Late Cenozoic environmental change in the Linxia Basin, Gansu, China as indicated by mammalian cenograms. Vertebrata PalAsiatica 47 (4), 282–298.
Deng, Q.D., Feng, X.Y., Zhang, P.Z., Xu, X.W., Yang, X.P., Peng, S.Z., Li, J., 2000. Active Tectonics of the Tianshan Mountains. Seismology Press, Beijing, p. 399 (in Chinese).
Ding, Z.L., Sun, J.M., Liu, T.S., Zhu, R.X., Yang, S.L., Guo, B., 1998. Wind-blown origin of the Pliocene red clay formation in the central Loess Plateau, China. Earth and Planetary Science Letters 161, 135–143.
Ding, L., Kapp, P., Zhong, D.L., Deng, W., 2003. Cenozoic volcanism in Tibet: evidence for a transition from oceanic to continental subduction. Journal of Petrology 44 (10), 1833–1865.
Dupont-Nivet, G., Krijgsman, W., Langereis, C.G., Abels, H.A., Dai, S., Fang, X.M., 2007. Tibetan plateau aridification linked to global cooling at the Eocene–Oligocene transition. Nature 445, 635–638.
Erdei, B., Hably, L., Kázmér, M., Utescher, T., Bruch, A.A., 2007. Neogene flora and vegetation development of the Pannonian domain in relation to palaeoclimate and palaeogeography. Palaeogeography, Palaeoclimatology, Palaeoecology 253, 115–140.
Eronen, J.T., Puolamäki, K., Liu, L., Lintulaakso, K., Damuth, J., Janis, C., Fortelius, M., 2010. Precipitation and large herbivorous mammals II: application to fossil data. Evolutionary Ecology Research 12, 235–248.
Fang, X.M., Garzione, C., Van der Voo, R., Li, J.J., Fan, M.J., 2003. Flexural subsidence by 29 Ma on the NE edge of Tibet from the magnetostratigraphy of Linxia Basin, China. Earth and Planetary Science Letters 210 (3–4), 545–560.
Fang, X.M., Yan, M.D., Van der Voo, R., Rea, D.R., Song, C.H., Pare's, J.M., Gao, J.P., Nie, J.S., Dai, S., 2005. Late Cenozoic deformation and uplift of the NE Tibetan plateau: evidence from high resolution magnetostratigraphy of the Guide Basin, Qinghai Province, China. Geological Society of America Bulletin 107, 1208–1225.
Fang, X.M., Zhao, Z.J., Li, J.J., et al., 2004. Magnetostratigraphy of the late Cenozoic Laojunmiao anticline in the northern Qilian Mts. and its implication on the northern Tibet uplift. Science in China (series D) 34 (2), 97–106.
Fang, X.M., Zhang, W.L., Meng, Q.Q., Gao, J.J., Wang, X.M., King, J., Song, C.H., Dai, S., Miao, Y.F., 2007. High-resolution magnetostratigraphy of the Neogene Huaitoutala section in the eastern Qaidam Basin on the NE Tibetan Plateau, Qinghai Province, China and its implication on tectonic uplift of the NE Tibetan Plateau. Earth and Planetary Science Letters 258, 293–306.
Flower, B.P., Kennett, J.P., 1994. The middle Miocene climatic transition: East Antarctic ice sheet development, deep ocean circulation and global carbon cycling. Palaeogeography, Palaeoclimatology, Palaeoecology 108, 537–555.
Fluteau, F., Ramstein, G., Besse, J., 1999. Simulating the evolution of the Asian and African monsoons during the past 30 Myr using an atmospheric general circulation model. Journal of Geophysical Research 104, 11995–12018.
Fradkina, A.F., Grinenko, O.V., Laukhin, S.A., Nechaev, V.P., Andreev, A.A., Klimanov, V.A., 2005. Northeastern Asia. In: Velichko, A.A., Nechaev, V.P. (Eds.), Cenozoic Climate And Environmental Changes in Russia: Special Paper — Geological Society of America, 382, pp. 105–120.
Fu, B.H., Ninomiya, Y., Guo, J.M., 2010. Slip partitioning in the northeast Pamir–Tian Shan convergence zone. Tectonophysics 483, 344–364.
Gao, Y.X., 1962. On some problems of Asian monsoon. In: Gao, Y.X. (Ed.), Some Questions about the East Asian Monsoon. Chinese Science Press, Beijing, pp. 1–49.
George, A.D., Marshallsea, S.J., Wyrwoll, K.H., Chen, J., Lu, Y.C., 2001. Miocene cooling in the northern Qilian Shan, northeastern margin of the Tibetan Plateau, revealed by apatite fission-track and vitrinite-reflectance analysis. Geology 29 (10), 939–942.
Guo, Z.T., Liu, T.S., et al., 1998. Climate extremes in Loess of China coupled with the strength of deep-water formation in the North Atlantic. Global Planet Change 18, 113–128.
Guo, Z.T., Ruddiman, W.F., Hao, Q.Z., Wu, H.B., Qiao, Y.S., Zhu, R.X., Peng, S.Z., Wei, J.J., Yuan, B.Y., Liu, T.S., 2002. Onset of Asian desertification by 22 Myr ago inferred from loess deposits in China. Nature 416, 159–163.
Guo, Z.T., Peng, S.Z., Hao, Q.Z., Biscaye, P.E., An, Z.S., Liu, T.S., 2004. Late Miocene–Pliocene development of Asian aridification as recorded in the Red-Earth Formation in northern China. Global Planet Change 41, 135–145.
Guo, Z.T., Sun, B., Zhang, Z.S., Peng, S.Z., Xiao, G.Q., Ge, J.Y., Hao, Q.Z., Qiao, Y.S., Liang, M.Y., Liu, J.F., Yin, Q.Z., Wei, J.J., 2008. A major reorganization of Asian climate by the early Miocene. Climate of the Past 43, 153–174.
Harris, N.B.W., 2006. The elevation history of the Tibetan Plateau and its implications for the Asian monsoon. Palaeogeography, Palaeoclimatology, Palaeoecology 241, 4–15.
Held, I.M., Soden, B.J., 2006. Robust responses of the hydrological cycle to global warming. Journal of Climate 19 (21), 5686–5699.
Heller, F., Liu, T.S., 1982. Magnetostratigraphical dating of loess deposits in China. Nature 300, 431–433.
Heller, F., Liu, T.S., 1984. Magnetism of Chinese loess deposits. Geophysical Journal of the Royal Astronomical Society 77, 125–141.
Hendrix, M.S., Dumitru, T.A., Graham, S.A., 1994. Late Oligocene–early Miocene unroofing in the Chinese Tian Shan: an early effect of the India–Asia collision. Geology 22, 487–490.
Hodges, K.V., Parish, R.R., Searle, M.P., 1996. Tectonic evolution of the central Annapurna Range, Nepalese Himalayas. Tectonics 15 (6), 1264–1291.
Hoorn, C., Ohja, T., Quade, J., 2000. Palynological evidence for vegetation development and climatic change in the Sub-Himalayan Zone, Neogene, Central Nepal. Palaeogeography, Palaeoclimatology, Palaeoecology 163 (3–4), 133–161.
Hou, Z.F., Zhang, J., Song, C.H., Li, J.J., Liu, J., Liu, S.P., Hui, Z.C., Peng, T.J., 2011. The oxygen and carbon isotopic records of Miocene sediments in the Tianshui Basin of the Northeastern Tibetan Plateau and their paleoclimatic implications. Marine Geology & Quaternary Geology 31 (3), 69–78 (in Chinese with English abstract).
Hu, Z., Sarjeant, W.A.S., 1992. Cenozoic spore-pollen assemblage zones from the shelf of the East China Sea. Review of Palaeobotany and Palynology 72 (1–2), 103–118.
Huang, C.B.C., Piper, J.D.A., Peng, S.T., Liu, T., Li, Z., Wang, Q.C., Zhu, R.X., 2006. Magnetostratigraphic study of the Kuche depression, Tarim Basin, and Cenozoic uplift of the Tian Shan Range, Western China. Earth and Planetary Science Letters 251, 346–364.
Hubert-Ferrari, A., Suppe, J., Gonzalez-Mieres, R., Wang, X., 2007. Mechanisms of active folding of the landscape, southern Tian Shan, China. Journal of Geophysical Research 112, B03S09. doi:10.1029/2006JB004362.
Hui, Z., Li, J.J., Xu, Q.H., Song, C.H., Zhang, J., Wu, F.L., Zhao, Z.J., 2011. Miocene vegetation and climatic changes reconstructed from a sporopollen record of the Tianshui Basin, NE Tibetan Plateau. Palaeogeography, Palaeoclimatology, Palaeoecology 308, 373–382.
Ivanov, D., Utescher, T., Mosbrugger, V., Syabryaj, S., Djordjević-Milutinović, D., Molchanoff, S., 2011. Miocene vegetation and climate dynamics in Eastern and Central Paratethys, Southeastern Europe. Palaeogeography, Palaeoclimatology, Palaeoecology 304, 262–275.
Jiang, H.C., Ding, Z.L., 2008. A 20 Ma pollen record of East-Asian summer monsoon evolution from Guyuan, Ningxia, China. Palaeogeography, Palaeoclimatology, Palaeoecology 265, 30–38.
Jiang, H.C., Ding, Z.L., 2010. Eolian grain-size signature of the Sikouzi lacustrine sediments (Chinese Loess Plateau): implications for Neogene evolution of the East Asian winter monsoon. GSA Bulletin 122 (5/6), 843–854.
Jiang, H.C., Ding, Z.L., Xiong, S.F., 2007. Magnetostratigraphy of the Neogene Sikouzi section at Guyuan, Ningxia, China. Palaeogeography, Palaeoclimatology, Palaeoecology 243, 223–234.
Jiménez-Moreno, G., Fauquette, S., Suc, J.P., 2008. Vegetation, climate and palaeoaltitude reconstructions of the Eastern Alps during the Miocene based on pollen records from Austria, Central Europe. Journal of Biogeography 35, 1638–1649.
Jiménez-Moreno, G., Suc, J.P., Fauquette, S., 2010. Miocene to Pliocene vegetation reconstruction and climate estimates in the Iberian Peninsula from pollen data. Review of Palaeobotany and Palynology 162, 403–415.
Jin, X.C., Wang, J., Chen, B.W., Ren, L.D., 2003. Cenozoic depositional sequences in the piedmont of the west Kunlun and their paleogeographic and tectonic implications. Journal of Asian Earth Sciences 21 (7), 755–765.
Korotky, A.M., Volkov, V.G., Grebennikova, T.A., Razzhigaeva, N.G., Pushkar, V.S., Ganzei, L.A., Mokhova, L.M., 2005. Far East. In: Velichko, A.A., Nechaev, V.P. (Eds.), Cenozoic Climate and Environmental Changes in Russia: Special Paper — Geological Society of America, 382, pp. 121–137.
Krijgsman, W., Garcés, M., Langereis, C.G., Daams, R., Van Dam, J., Van Der Meulen, A.J., Agustí, J., Cabrera, L., 1996. A new chronology for the middle to late Miocene continental record in Spain. Earth and Planetary Science Letters 142 (3–4), 367–380.
Kukla, G., Heller, F., Liu, X.M., Xu, T.C., Liu, T.S., An, Z.S., 1988. Pleistocene climates in China dated by magnetic susceptibility. Geology 16, 811–814.
Kutzbach, J.E., Guetter, P.J., Ruddiman, W.F., Prell, W.L., 1989. Sensitivity of climate to late Cenozoic uplift in southern Asia and the American west: numerical experiments. Journal of Geophysical Research 94 (D15), 18393–18407.
Larsson, L.M., Dybkjær, K., Rasmussen, E.S., Piasecki, S., Utescher, T., Vajd, V., 2011. Miocene climate evolution of northern Europe: a palynological investigation from Denmark. Palaeogeography, Palaeoclimatology, Palaeoecology 309, 161–175.
Leloup, P.H., Lacassin, R., Tapponnier, P., Schärer, U., Zhong, D.L., Liu, X.H., 1995. The Ailao Shan-Red River shear zone (Yunnan, China), Tertiary transform boundary of Indochina. Tectonophysics 251, 3–10.
Li, J.J., Fang, X.M., 1999. Uplift of the Tibetan Plateau and environmental changes. Chinese Science Bulletin 44, 2117–2124.
Li, J.J., Fang, X.M., Zhu, J.J., 1995. Paleomagnetic chronology and type sequence of the Cenozoic stratigraphy of the Linxia Basin in Gansu Province of China. Annual Research Report on Geological Evolution, Environment Changes and Ecotope of Qinghai-Xizang Plateau. Science Press, Beijing, pp. 41–53.
Li, J.G., Jiang, L., Zhang, Y.Y., Wang, J.P., 2003. Neogene palynofloral successions from Taibei Depression in southwestern continent shelf of the East China Sea. Acta Palaeontologica Sinica 42, 239–256 (in Chinese with English abstract).
Li, J.J., Zhang, J., Song, C.H., Zhao, Z.J., Zhang, Y., Wang, X.X., Zhang, J.M., Cui, Q.Y., 2006. Miocene Bahean stratigraphy in the Longzhong Basin, northern central China and its implications. Science in China (series D) 49 (12), 1270–1279.
Liang, M.Y., Guo, Z.T., Kahmann, A.J., Oldfield, F., 2009. Geochemical characteristics of the Miocene eolian deposits in China: their provenance and climate implications. Geochemistry, Geophysics, Geosystems 10, Q04004. doi:10.1029/2008GC002331.
Lin, X.B., Chen, H.L., Wyrwoll, K.H., Cheng, X.G., 2010. Commencing uplift of the Liupan Shan since 9.5 Ma: evidences from the Sikouzi section at its east side. Journal of Asian Earth Sciences 37, 350–360.
Liu, T.S., 1985. Loess and the Environment. China Ocean Press, Beijing. (pp. 1–251).
Liu, T.S., 1986. Loess and the Environment. China Ocean Press, Beijing.

Liu, T.S., Ding, Z.L., 1998. Chinese loess and the paleomonsoon. Annual Review of Earth and Planetary Sciences 26, 111–145.
Liu, T.S., Guo, Z.T., 1997. Geological Environment in China and Global Change. In: An, Z.S. (Ed.), Selected Works of Liu Tungsheng. Science Press, Beijing, pp. 192–202.
Liu, T.S., Zheng, M.P., Guo, Z.T., 1998. Initiation and evolution of the Asian monsoon system timely coupled with the ice-sheet growth and the tectonic movements in Asia. Quaternary Sciences 3, 194–204 (in Chinese).
Liu, X.D., Kutzbach, J.E., Liu, Z., et al., 2003. The Tibetan Plateau as amplifier of orbital scale variability of the East Asian monsoon. Geophysical Research Letters 30 (16), 1839. doi:10.1029/2003GL017510.
Liu, J.F., Guo, Z.T., Qiao, Y.S., Hao, Q.Z., Yuan, B.Y., 2006. Eolian origin of the Miocene loess-soil sequence at Qin'an, China: evidence of quartz morphology and quartz grain-size. Chinese Science Bulletin 51 (2), 213–220.
Liu, Y.S., Utescher, T., Zhou, Z.K., Sun, B.N., 2011. The evolution of Miocene climates in North China: preliminary results of quantitative reconstructions from plant fossil records. Palaeogeography, Palaeoclimatology, Palaeoecology 304, 308–317.
Lu, H.J., Xiong, S.F., 2009. Magnetostratigraphy of the Dahonggou section, northern Qaidam Basin and its bearing on Cenozoic tectonic evolution of the Qilian Shan and Altyn Tagh Fault. Earth and Planetary Science Letters 288, 539–550.
Lu, H.Y., Wang, X.Y., An, Z.S., Miao, X.D., Zhu, R.X., Ma, H.Z., Li, Z., Tan, H.B., Wang, X.Y., 2004. Geomorphologic evidence of phased uplift of the northeastern Qinghai-Tibetan Plateau since 14 million years. Science in China (series D) 47 (9), 822–833.
Lu, H.Y., Wang, X., Li, L., 2010. Aeolian sediment evidence that global cooling has driven late Cenozoic stepwise aridification in central Asia. Geological Society of London. Special Publication 342, 29–44.
Ma, Y.Z., Li, J.J., Fan, X.M., 1998. Pollen-based vegetational and climatic records during 30.6 to 5.0 My from Linxia area, Gansu. Chinese Science Bulletin 43 (3), 301–304 (in Chinese).
Ma, Y.Z., Fang, X.M., Li, J.J., Wu, F.L., Zhang, J., 2005. The vegetation and climate change during Neocene and Early Quaternary in Jiuxi Basin, China. Science in China (series D) 48 (5), 676–688.
Manabe, S., Broccoli, A.J., 1990. Mountains and arid climates of middle latitudes. Science 247, 192–194.
Manabe, S., Terpstra, T.B., 1974. The effects of mountains on the general circulation of the atmosphere as identified by numerical experiments. Journal of Atmospheric Sciences 31, 3–42.
Miao, Y.F., Fang, X.M., Herrmann, M., Wu, F.L., Liu, D.L., 2011a. Miocene pollen record of KC-1 core in the Qaidam Basin, NE Tibetan Plateau and implications for evolution of the East Asian monsoon. Palaeogeography, Palaeoclimatology, Palaeoecology 299, 30–38.
Miao, Y.F., Meng, Q.Q., Fang, X.M., Yan, X.L., Wu, F.L., Song, C.H., 2011b. Origin and development of Artemisia (Asteraceae) in Asia and its implications for the uplift history of the Tibetan Plateau: a review. Quaternary International 236 (1–2), 3–12.
Micheels, A., Bruch, A.A., Eronen, J., Fortelius, M., Harzhauser, M., Utescher, T., Mosbrugger, V., 2011. Analysis of heat transport mechanisms from a Late Miocene model experiment with a fully-coupled atmosphere–ocean general circulation model. Palaeogeography, Palaeoclimatology, Palaeoecology 304, 337–350.
Mosbrugger, V., Utescher, T., 1997. The coexistence approach—a method for quantitative reconstructions of Tertiary terrestrial palaeoclimate data using plant fossils. Palaeogeography, Palaeoclimatology, Palaeoecology 134, 61–86.
Mosbrugger, V., Utescher, T., Dilcher, D.L., 2005. Cenozoic continental climatic evolution of central Europe. Proceedings of the National Academy of Sciences of the United States of America 102, 14964–14969.
Ohja, T.P., Butler, B., Quade, J., DeCelles, P., 2000. Magnetic polarity stratigraphy of the Neogene Siwalik Group at Khutia Khola, far western Nepal. Geological Society of America Bulletin 112 (3), 424–434.
Passey, B.H., Ayliffe, L.K., Kaakinen, A., Zhang, Z., Eronen, J.T., Zhu, Y., Zhou, L., Cerling, T.E., Fortelius, M., 2009. Strengthened East Asian summer monsoons during a period of high-latitude warmth? Isotopic evidence from Mio-Pliocene fossil mammals and soil carbonates from northern China. Earth and Planetary Science Letters 277, 443–452.
Popova, S.V., Rögl, F., Rozanov, A.Y., Steininger, F.F., Shcherba, I.G., Kovac, M., 2004. Lithological-Paleogeographic maps of Paratethys — 10 maps Late Eocene to Pliocene. Courier Forschungsinstitut Senckenberg 250. 46 pp. 10 maps. Frankfurt/Main.
Popova, S., Utescher, T., Gromyko, D., Bruch, A.A., Mosbrugger, V., 2011. Palaeoclimate evolution in Siberia and the Russian Far East from the Oligocene to Pliocene—evidence from fruit and seed floras. Turkish Journal of Earth Sciences. doi:10.3906/yer-1005-6.
Qiang, X.K., An, Z.S., Song, Y.G., Chang, H., Sun, Y.B., Liu, W.G., AO, H., Dong, J.B., Fu, C.F., Wu, F., 2011. New Eolian red clay sequence on the western Chinese Loess Plateau linked to onset of Asian desertification about 25 Ma ago. Science in China (series D) 54, 136–144.
Quade, J., Cerling, T.E., Bowman, J.R., 1989. Development of Asian monsoon revealed by marked ecological shift during the latest Miocene in the northern Pakistan. Nature 342, 163–166.
Quade, J., Cater, M.L.J., Ojha, P.T., Adam, J., Harrison, M.T., 1995. Late Miocene environmental change in Nepal and the northern Indian subcontinent: stable isotopic evidence from paleosols. Geological Society of America Bulletin 107, 1381–1397.
Quade, J., Breecker, D.O., Daeron, M., Eiler, J., 2011. The paleoaltimetry of Tibet: an isotopic perspective. American Journal of Science 311 (2), 77–115.
Ramstein, G., Fluteau, F., Besse, J., Joussaume, S., 1997. Effect of orogeny, plate motion and land-sea distribution on Eurasian climate change over the past 30 million years. Nature 386, 788–795.
Raymo, M.E., Ruddiman, W.F., 1992. Tectonic forcing of late Cenozoic climate. Nature 359, 117–120.
Ritts, B.D., Yue, Y., Graham, S.A., Sobel, E.R., Abbink, O.A., Stockli, D., 2008. From sea level to high elevation in 15 million years: uplift history of the northern Tibetan Plateau margin in the Altun Shan. American Journal of Science 308, 657–678.
Rögl, V.F., 1998. Palaeogeographic Considerations for Mediterranean and Paratethys Seaways (Oligocene to Miocene). Annalen des Naturhistorischen Museums Wien 99 A, 279–310.
Rögl, F., 1999. Mediterranean and Paratethys. Facts and hypotheses of an Oligocene to Miocene paleogeography. Geologica Carpathica 50, 339–349.
Rögl, F., Steininger, F.F., 1983. Vom Zerfall der Tethys zu Mediterran und Paratethys. Die Neogene Palaeogeographie und Palinspastik des zirkum-mediterranen Raumes. Annalen des Naturhistorischen Museums Wien 85, 135–163 (Wien).
Rowley, D.B., Currie, B.S., 2006. Palaeo-altimetry of the late Eocene to Miocene Lunpola Basin, central Tibet. Nature 439, 677–681.
Rowley, D.B., Garzione, C.N., 2007. Stable isotope-based paleoaltimetry. Annual Review of Earth and Planetary Sciences 35, 463–508.
Ruddiman, W.F., 2002. Earth's Climate: Past and Future. W. H. Freeman and Company, New York. (pp. 1–465).
Ruddiman, W.F., Kutzbach, J.E., 1989. Forcing of the late Cenozoic uplift northern hemisphere climate by plateau uplift in the Southern Asia and American West. Journal of Geophysical Research 94, 18409–18427.
Sanyal, P., Bhattacharya, S.K., Kumar, R., Ghosh, S.K., Sangode, S.J., 2004. Mio-Pliocene monsoonal record from Himalayan Foreland basin-Indian Siwalik and its relation to the vegetational change. Palaeogeography, Palaeoclimatology, Palaeoecology 205, 23–41.
Sanyal, P., Bhattacharya, S.K., Prasad, M., 2005. Chemical diagenesis of Siwalik sandstone: isotopic and mineralogical proxies from Surai Khola section, Nepal. Sedimentary Geology 180, 57–74.
Schulz, H.M., Vakarcs, G., Magyar, I., 2005. The birth of the Paratethys during the Early Oligocene: from Tethys to an ancient Black Sea analogue? Global Planet Change 49 (3–4), 163–176.
Singh, G., 1988. History of aridland vegetation and climate: a global perspective. Biological Reviews 63, 159–195.
Sobel, E.R., Chen, J., Heermance, R.V., 2006. Late Oligocene–Early Miocene initiation of shortening in the Southwestern Chinese Tian Shan: implications for Neogene shortening rate variations. Earth and Planetary Science Letters 247, 70–81.
Song, C.H., Fang, X.M., Li, J.J., Gao, J.P., Zhao, Z.J., Fan, M.J., 2001a. Tectonic uplift and sedimentary evolution of the Jiuxi Basin in the northern margin of the Tibetan Plateau since 13 Ma BP. Science in China (series D) 44 (Suppl), 192–202.
Song, Y.G., Fang, X.M., Li, J.J., An, Z.S., Miao, X.D., 2001b. The late Cenozoic uplift of Liupan Shan, China. Science in China (series D) 44 (suppl), 176–184.
Song, X.Y., Spicer, R.A., Yang, J., Yao, Y.F., Li, C.S., 2010. Pollen evidence for an Eocene to Miocene elevation of central southern Tibet predating the rise of the High Himalaya. Palaeogeography, Palaeoclimatology, Palaeoecology 297, 159–168.
Spicer, R.A., Harris, N.B.W., Widdowson, M., Herman, A.B., Guo, S., Valdes, S., Wolf, J., Kelley, S., 2003. Constant elevation of southern Tibet over the past 15 million years. Nature 421, 622–624.
Sun, J.M., Liu, T.S., 2006. The age of the Taklimakan Desert. Science 312, 1621.
Sun, X.J., Wang, P.X., 2005. How old is the Asian monsoon system—palaeobotanical records from China. Palaeogeography, Palaeoclimatology, Palaeoecology 222, 181–222.
Sun, J.M., Zhang, Z.Q., 2008. Palynological evidence for the Mid-Miocene climatic optimum recorded in Cenozoic sediments of the Tianshan Range, northwestern China. Global Planet Change 64, 53–68.
Sun, J.M., Zhang, Z.Q., 2009. Syntectonic growth strata and implications for late Cenozoic tectonic uplift in the northern Tian Shan, China. Tectonophysics 463, 60–68.
Sun, D.H., John, S., An, Z.S., Chen, M.Y., Yue, L.P., 1998. Magnetostratigraphy and paleoclimatic interpretation of a continuous 7.2 Ma Late Cenozoic eolian sediments from the Chinese Loess Plateau. Geophysical Research Letters 25, 85–88.
Sun, J.M., Zhu, R.X., Bowler, J., 2004. Timing of the Tianshan Mountains uplift constrained by magnetostratigraphic analysis of molasse deposits. Earth and Planetary Science Letters 219, 239–253.
Sun, J.M., Xu, Q.H., Huang, B.C., 2007. Late Cenozoic magnetochronology and paleoenvironmental changes in the northern foreland basin of the Tian Shan Mountains. Journal of Geophysical Research 112. doi:10.1029/2006JB004653.
Sun, J.M., Li, Y., Zhang, Z.Q., Fu, B.H., 2009. Magnetostratigraphic data on the Neogene growth folding in the foreland basin of the southern Tianshan Mountains. Geology 37, 1051–1054.
Sun, D.H., Bloemendal, J., Yi, Z.Y., Zhu, Y.H., Wang, X., Zhang, Y.B., Li, Z.J., Wang, F., Han, F., Zhang, Y., 2011. Palaeomagnetic and palaeoenvironmental study of two parallel sections of late Cenozoic strata in the central Taklimakan Desert: implications for the desertification of the Tarim Basin. Palaeogeography, Palaeoclimatology, Palaeoecology 300, 1–10.
Syabryaj, S., Utescher, T., Molchanoff, S., Bruch, A.A., 2007. Vegetation and palaeoclimate in the Miocene of Ukraine. Palaeogeography, Palaeoclimatology, Palaeoecology 253 (1–2), 153–168.
Tang, Z.H., Ding, Z.L., White, P.D., Dong, X.X., Ji, J.L., Jiang, H.C., Luo, P., Wang, X., 2011. Late Cenozoic central Asian drying inferred from a palynological record from the northern Tian Shan. Earth and Planetary Science Letters 302 (3–4), 439–447.
Utescher, T., Mosbrugger, V., Ashraf, A., 2000. Terrestrial climate evolution in Northwest Germany over the last 25 million years. Palaios 15, 430–449.
Utescher, T., Djordjevic-Milutinovic, D., Bruch, A., Mosbrugger, V., 2007a. Palaeoclimate and vegetation change in Serbia during the last 30 Ma. Palaeogeography, Palaeoclimatology, Palaeoecology 253 (1–2), 141–152.
Utescher, T., Erdei, B., Francois, L., Mosbrugger, V., 2007b. Tree diversity in the Miocene forests of Western Eurasia. Palaeogeography, Palaeoclimatology, Palaeoecology 253 (1–2), 226–250.
Utescher, T., Mosbrugger, V., Ivanov, D., Dilcher, D.L., 2009. Present-day climatic equivalents of European Cenozoic climates. Earth and Planetary Science Letters 284 (3–4), 544–552.
Van Dam, J.A., 2006. Geographic and temporal patterns in the late Neogene (12–3 Ma) aridification of Europe. The use of small mammals as paleoprecipitation proxies. Palaeogeography, Palaeoclimatology, Palaeoecology 238, 190–218.

Vandenberghe, J., Lu, H.Y., Sun, D.H., 2004. The late Miocene and Pliocene climate in East Asia as recorded by grain size and magnetic susceptibility of the Red Clay deposits, Chinese loess Plateau. Palaeogeography, Palaeoclimatology, Palaeoecology 204, 239–255.

Velichko, A.A., Akhlestina, E.F., Borisonva, O.K., et al., 2005. East European Plain. In: Velichko, A.A., Nechaev, V.P. (Eds.), Cenozoic Climate and Environmental Changes in Russia: Special Paper — Geological Society of America, 382, pp. 31–66.

Wan, S.M., Li, A.C., Peter, D., Clift, J., Stuut, W., 2007. Development of the East Asian monsoon: mineralogical and sedimentologic records in the northern South China Sea since 20 Ma. Palaeogeography, Palaeoclimatology, Palaeoecology 152, 37–47.

Wan, S.M., Clift, P.D., Li, A.C., Li, T.G., Yin, X.Y., 2010. Geochemical records in the South China Sea: implications for East Asian summer monsoon evolution over the last 20 Ma. Geological Society of London. Special Publication 342, 245–263.

Wang, P.X., 1984. Progress in Late Cenozoic Palaeoclimatology of China: A Brief Review. In: Whyte, R.O., Chiu, T.N., Leung, C.K., So, C.L. (Eds.), The Evolution of the East Asian Environment. Hong Kong, Center of Asian Studies, University of Hong Kong, pp. 165–187.

Wang, W.M., 1996. A sequence of changes on Neogene pollen floras and environmental events of north China-comprehensive study of core and outcrop sections. Post-Doctorate Reports (unpublished), Nanjing, pp. 1–60 (in Chinese).

Wang, S.J., Gao, C.H., 1990. The formation and evolution of the arid environment of the inland Tarim basin since late Ceonozoic era. Quaternary Sciences 4, 372–380 (in Chinese).

Wang, P.X., Prell, W.L., Blum, P., 2000. Proceedings of the ocean drilling program, initial reports, 184 [CD-ROM]. Available from: Ocean Drilling Program, Texas A & M University, College Station, TX 77845–9547, USA, pp. 1–77.

Wang, W.M., Saito, T., Nakagawa, T., 2001. Palynostratigraphy and climatic implications of Neogene deposits in the Himi area of Toyama Prefecture, Central Japan. Review of Palaeobotany and Palynology 117 (4), 281–295.

Wang, P.X., Jian, Z.M., Zhao, Q.H., Li, Q.Y., Wang, L.J., Liu, Z.F., et al., 2003. Deep-sea records of the evolution of the South China Sea and the East Asian monsoon. Chinese Science Bulletin 48 (21), 2228–2239.

Wang, X.Y., Lu, H.Y., Ji, J.F., Wang, X.Y., Zhao, J.B., Huang, B.C., Li, Z., 2006. Origin of the Red Earth sequence on the northeastern Tibetan Plateau and its implications for regional aridity since the middle Miocene. Science in China (series D) 49, 505–517.

Wang, J.Y., Fang, X.M., Zhang, W.L., Zan, J.B., Miao, Y.F., 2010. Magnetostratigraphy and its implications of the Heilinding section, the Linxia Basin, Gansu Province, China. Marine Geology & Quaternary Geology 30 (5), 129–135 (Chinese with English abstract).

Wang, W.T., Zhang, P.Z., Kirby, E., Wang, L.H., Zhang, G.L., Zheng, D.W., Chai, C.Z., 2011a. A revised chronology for Tertiary sedimentation in the Sikouzi basin: implications for the tectonic evolution of the northeastern corner of the Tibetan Plateau. Tectonophysics 505, 100–114.

Wang, X.X., Zattin, M., Li, J.J., Song, C.H., Peng, T.J., Liu, S.P., Liu, B., 2011b. Eocene to Pliocene exhumation history of the Tianshui–Huicheng region determined by Apatite fission track thermochronology: implications for evolution of the northeastern Tibetan Plateau margin. Journal of Asian Earth Sciences 42, 97–110.

Wang, Z.C., Zhang, P., Garzione, C.N., Lease, R.O., Zhang, G.L., Zheng, D.W., Brian, H., Yuan, D.Y., Li, C.Y., Liu, J.H., Wu, Q.L., 2011c. Magnetostratigraphy and depositional history of the Miocene Wushan basin on the NE Tibetan plateau, China: implications for middle Miocene tectonics of the West Qinling fault zone. Journal of Asian Earth Sciences. doi:10.1016/j.jseaes.2011.06.009.

Wei, G.J., Li, X.H., Liu, Y., Shao, L., Liang, X.R., 2006. Geochemical record of chemical weathering and monsoon climate change since the early Miocene in the South China Sea. Paleoceanography 21 (4), 1–11.

White, J.M., Ager, T.A., Adam, D.P., Leopold, E.B., Liu, G., Jetté, H., Schweger, C.E., 1997. An 18 million year record of vegetation and climate change in northwestern Canada and Alaska: tectonic and global climatic correlates. Palaeogeography, Palaeoclimatology, Palaeoecology 130, 293–306.

Wolfe, J.A., 1994. An analysis of Neogene climates in Beringia. Palaeogeography, Palaeoclimatology, Palaeoecology 108, 207–216.

Xu, R., 1978. On the palaeobotanical evidence for continental drift and Himalayan uplift. Palaeobotanist 25, 131–142 (in Chinese).

Yabe, A., 2008. Early Miocene terrestrial climate inferred from plant megafossil assemblages of the Joban and Soma areas, Northeast Honshu, Japan. Bulletin. Geological Survey 59 (7/8), 397–413.

Yi, S., Batten, D.J., Yun, H., Park, S.J., 2003. Cretaceous and Cenozoic non-marine deposits of the Northern South Yellow Sea Basin, offshore western Korea: palynostratigraphy and palaeoenvironments. Palaeogeography, Palaeoclimatology, Palaeoecology 191, 15–44.

Yin, A., Harrison, T.M., Ryerson, F.J., Chen, W., Kidd, W.S.F., Copeland, P., 1994. Tertiary structural evolution of Gangdeses thrust system, Southeastern Tibet. Journal of Geophysical Research 99, 18175–18201.

Yin, A., Nie, S., Craig, P., Harrison, T.M., Ryerson, F.J., Qian, X., Yang, G., 1998. Late Cenozoic tectonic evolution of the southern Chinese Tian Shan. Tectonics 17, 1–27.

Zachos, J.C., Pagani, M., Sloan, L., Thomas, E., Billups, K., 2001. Trends, rhythms, and aberrations in global climate 65 Ma to present. Science 292, 686–693.

Zachos, J.C., Gerald, R.D., Richard, E.Z., 2008. An early Cenozoic perspective on greenhouse: warming and carbon-cycle dynamics. Nature 451 (17), 279–283.

Zhang, L.Y., 1981. The influences of the uplift of Qinghai-Xizang Plateau on the Quaternary environmental evolution in China. Journal of Lanzhou University (Natural Science) 3, 142–155 (in Chinese).

Zhang, Z.S., Guo, Z.T., 2005. Spatial character reconstruction of different periods in 670 Oligocene and Miocene. Quaternary Sciences 25 (4), 523–530 (in Chinese with English abstract).

Zhang, Z.Q., Sun, J.M., 2011. Palynological evidence for Neogene environmental change in the foreland basin of the southern Tianshan range, northwestern China. Global Planet Change 75, 56–66.

Zhang, Z.S., Wang, H.J., Guo, Z.T., Jiang, D.B., 2007. What triggers the transition of palaeoenvironmental patterns in China, the Tibetan Plateau uplift or the Paratethys Sea retreat? Palaeogeography, Palaeoclimatology, Palaeoecology 245, 317–331.

Zheng, D.W., Zhang, P.Z., Wan, J.L., Yuan, D.Y., Li, C.Y., Yin, G.M., Zhang, G.L., Wang, Z.C., Min, W., Chen, J., 2006. Rapid exhumation at 8 Ma on the Liupan Shan thrust fault from apatite fission-track thermochronolgy: implications for growth of the northeastern Tibetan Plateau margin. Earth and Planetary Science Letters 248, 198–208.